***N*-chlorination mediates protective and immunomodulatory effects of oxidized human plasma proteins**

Running title: Effects of *N*-chlorinated plasma proteins

Agnes Ulfig, Anton V. Schulz, Alexandra Müller, Natalie Lupilov, and Lars I. Leichert

Ruhr University Bochum, Institute of Biochemistry and Pathobiochemistry – Microbial Biochemistry, Universitätsstrasse 150, 44780 Bochum, Germany

Correspondence: Lars I. Leichert
Ruhr University Bochum
Institute of Biochemistry and Pathobiochemistry
Microbial Biochemistry
Universitätsstrasse 150
44780 Bochum, Germany
Phone: +49 234 3224585
Fax: +49 234 3214332
E-mail: lars.leichert@ruhr-uni-bochum.de

ABSTRACT

Hypochlorous acid (HOCl), a powerful antimicrobial oxidant, is produced by neutrophils to fight infections. Here we show that *N*-chlorination, induced by HOCl concentrations encountered at sites of inflammation, converts blood plasma proteins into chaperone-like holdases that protect other proteins from aggregation. This chaperone-like conversion was reversible by antioxidants and was abrogated by prior methylation of basic amino acids. Furthermore, reversible *N*-chlorination of basic amino acid side chains is the major factor that converts plasma proteins into efficient activators of immune cells. Finally, HOCl-modified serum albumin was found to act as a pro-survival molecule that protects neutrophils from cell death induced by highly immunogenic foreign antigens. We propose that activation and enhanced persistence of neutrophils mediated by HOCl-modified plasma proteins, resulting in the increased and prolonged generation of ROS, including HOCl, constitutes a potentially detrimental positive feedback loop that can only be attenuated through the reversible nature of the modification involved.

35 **INTRODUCTION**

36 Recruitment and activation of neutrophils at sites of infection is considered one of the principal
37 mechanisms by which the human body protects itself against diseases. The killing strategy of
38 neutrophils involves the ingestion of pathogens into the phagosome, accompanied by the
39 production of a diverse set of so-called reactive oxygen species (ROS), including superoxide
40 anions ($O_2^{\cdot-}$), hydrogen peroxide (H_2O_2) and hypochlorous acid (HOCl) in a process known as
41 the respiratory burst (recently reviewed in refs. [1,2]).

42 HOCl, a major inflammatory ROS, is produced from hydrogen peroxide and chloride ions by
43 the heme enzyme myeloperoxidase (MPO) [3,4]. The antimicrobial properties of HOCl are well
44 documented and numerous reports have provided strong evidence for severe damage to
45 bacterial components within the neutrophil phagosome [5–7].

46 A particularly important target of HOCl are proteins. In proteins, HOCl exposure typically leads
47 to side chain modification [8–12], fragmentation [13,14], misfolding/aggregation [15] or
48 intermolecular di-tyrosine cross-linking, a hallmark of HOCl-oxidized proteins [16]. This often
49 leads to their aggregation [17–19]. Consequently, various mechanisms to counter the accumulation
50 of these misfolded proteins under HOCl stress exist in bacteria. These are mediated by
51 chaperones that are activated by HOCl, the very same reactive species they protect against. One
52 of the first protective proteins to be noticed was Hsp33, which gets reversibly activated by
53 HOCl through oxidation of four critical cysteine residues [19]. This is not surprising, as cysteine
54 thiols together with methionine residues react rapidly with HOCl [20,21]. More recently, we found
55 that *E. coli* RidA, a member of the highly conserved, but functionally diverse
56 YjgF/YER057c/UK114 protein family, also undergoes HOCl-based conversion into a
57 chaperone holdase. This chaperone was highly active as protector of proteins from HOCl-
58 induced aggregation. However in this case, instead of cysteine oxidation, *N*-chlorination of
59 basic amino acids was the mechanism of its activation [17], although reactivity of HOCl with side
60 chains of lysine and arginine is four to seven orders of magnitude lower than that of cysteine

[22]. But much like cysteine oxidation, *N*-chlorination is a reversible oxidative modification that can be removed by cellular antioxidants such as ascorbate, glutathione or thioredoxin and thus can switch the holdase function of RidA off [17,23,24].

Similar observations were made more recently with *E. coli* CnoX (YbbN) that, when activated via *N*-chlorination, binds to and prevents a variety of substrates from aggregation and being irreversible oxidized [25].

While HOCl is highly bactericidal, generation of HOCl by immune cells is not without risk to the human body itself (reviewed in refs. [26–29]). During inflammatory processes, up to 30% of total cellular MPO is secreted by neutrophils into extracellular surroundings via degranulation, leakage during phagocytosis, or by association with NETs [30]. Neutrophils, accumulated in the interstitial fluid of inflamed tissues, have been reported to generate HOCl at concentrations of up to 25-50 mM per hour [31]. It is thus not surprising that HOCl can also drastically increase the activity of the extracellular chaperone α_2-macroglobulin (α_2M) in human blood plasma to counteract the aggregation of host proteins under hypochlorous acid stress [32]. However, the underlying molecular mechanism of HOCl-mediated conversion of this plasma protein is still unclear.

And while neutrophils produce high amounts of HOCl, it does not accumulate at those levels, as it reacts instantly with diverse biological molecules including proteins, DNA [33], cholesterol [34] and lipids [35]. But due to their high abundance in blood and interstitial fluid, human serum albumin (HSA) and other plasma proteins are considered the major targets of HOCl-mediated damage and as such constitute the main sink for HOCl in the vicinity of inflammation [36–40]. The resulting products of the reaction of plasma proteins with hypochlorous acid, known as advanced oxidation protein products (AOPPs), have, therefore, been employed as *in vivo* markers of chronic inflammation [41]. Accumulation of AOPPs has been first discovered in patients with chronic kidney disease [41] and later also found in a variety of other inflammatory

86 diseases, e.g. cardiovascular disease, neurodegenerative disorders, rheumatoid arthritis and
87 some cancers (recently reviewed in ref. [42]).
88 To date, a number of studies have been carried out to elucidate the role of AOPPs in
89 inflammatory processes [43–46]. Accumulating experimental evidence supports a critical
90 contribution of AOPPs to the progression of inflammation [44]. HOCl-modifed HSA accumulates
91 in inflammatory diseases and was found to act as proinflammatory mediator by increasing
92 oxidative stress and inflammation through stimulation of leukocytes [46,47].
93 Based on these findings we hypothesized that reversible *N*-chlorination in response to HOCl-
94 stress could be the principal chemical modification contributing to the observed physiological
95 properties of AOPPs. Furthermore, as we observed in previous studies that the HSA homologue
96 bovine serum albumin (BSA) could be transformed into a chaperone-like holdase by HOCl-
97 treatment [17], we speculated that *N*-chlorination serves as general rather than specific mechanism
98 to transform certain proteins into a chaperone-like state.
99 Here, we study the effects of reversible *N*-chlorination on the function of human plasma
100 proteins. We show that, upon *N*-chlorination, not only α_2M, but all plasma fractions tested,
101 exhibit chaperone-like activity and as such could prevent the HOCl-induced formation of
102 protein aggregates at the site of inflammation. Moreover, exposure to HOCl at concentrations
103 present in chronically inflamed tissues turned the majority of plasma proteins into efficient
104 activators of neutrophil-like cells. Previous studies revealed that HOCl-treated HSA can
105 stimulate leukocytes to produce more ROS during inflammation [47,48]. Now we find that
106 reversible *N*-chlorination is the main chemical modification that mediates the activation of
107 NADPH oxidase-dependent ROS generation by immune cells by AOPPs. Finally, we show that
108 HOCl-modified HSA is a pro-survival factor for immune cells and protects neutrophils from
109 cell death by highly immunogenic antigens.

110 Our data strongly suggest that *in vivo* reversible *N*-chlorination of human plasma proteins not
111 only converts them into effective chaperone-like holdases but is also the principal mechanism
112 that turns these proteins into mediators of the innate immune system.

113 **MATERIAL AND METHODS**

114 **Preparation of plasma protein solutions**

115 Albumin from human serum (HSA, Product # A9511), human γ-globulins (Product # G4386),
116 immunoglobulin G from human serum (IgG, Product # I4506) Cohn fraction IV (Product #
117 G3637) and human whole serum (sterile-filtered from male AB plasma, Product # H4522) were
118 purchased from Sigma-Aldrich, St. Louis, USA, and used without further purification.
119 Protein stock solutions were freshly prepared by dissolving or diluting varying amounts of the
120 protein fractions in 1xPBS buffer, pH 7.4 (Gibco Life Sciences).

121 **Purification of α_2-macroglobulin**

122 α_2-Macroglobulin was purified from human plasma (obtained from Zen-Bio, Inc., North
123 Carolina, USA, Product # SER-SLP, Lot # 11108) by the method of Imber and Pizzo, 1981 [49]
124 with slight modifications. Briefly, 880 mL fresh-frozen human plasma were thawed on ice and
125 dialyzed against frequent changes of deionized water for 72 hours at 4 °C using a Spectra/Por
126 dialysis membrane with a MWCO of 12-14 kDa (Spectrum Laboratories Inc., Rancho
127 Dominguez, CA). Insoluble material was removed by centrifugation for 30 minutes at 10,000
128 x g and 4 °C. The supernatant plasma solution (200 mL) was then dialyzed for 24 hours at 4 °C
129 against 5 L 1xPBS pH 6.0. Metal chelate chromatography was performed at 4 °C using an
130 IMAC zinc-Sepharose 6 Fast Flow column (2.6 x 20 cm, GE Healthcare Life Sciences,
131 Amersham, UK) equilibrated with 1xPBS pH 6.0. Dialyzed plasma was applied to the column
132 and washed with 1xPBS pH 6.0 until the absorption at 280 nm of the eluant (measured with a
133 JASCO V-650 UV/VIS spectrophotometer (JASCO, Tokyo, Japan)) reached a value lower than
134 0.01. Bound protein was then eluted from the column with 0.01 M NaOAc, 0.15 M NaCl, pH
135 5.0. Peak protein fractions were combined and concentrated using Vivaspin 20 concentrators
136 with a MWCO of 100 kDa. Gel filtration of the concentrated protein pool fraction was
137 performed at 4 °C on a HiPrep 26/60 Sephacryl S-300 High resolution column (2.6 x 60 cm)
138 equilibrated with 1xPBS pH 7.4. High molecular weight peak fractions containing α_2-

139 macroglobulin were combined, concentrated and dialyzed against 1xPBS pH 7.4 containing
140 40% (v/v) glycerol. Aliquots were stored at -20° C.

141 **Determination of protein concentrations**

142 Protein concentration in g · L^{-1} of human serum was calculated using Pierce™ Bicinchoninic
143 Acid (BCA) Protein Assay Kit (Thermo Fisher Scientific, Waltham, Massachusetts, USA) with
144 bovine albumin as standard carried out following the manufacturer's instructions. To calculate
145 a molar concentration, an average molar mass of proteins of 66,357.12 Da was assumed (molar
146 mass of human serum albumin).

147 For HSA, IgG, the γ-globulin fraction, and α_2-macroglobulin, the concentration was determined
148 by measuring the absorbance at 280 nm (A_{280nm}) using a JASCO V-650 UV/VIS
149 spectrophotometer. The molar extinction coefficient used for HSA was ε_{280}= 35,700 M^{-1} cm^{-1}
150 [50]. Concentration of the γ-globulin fraction was estimated using the extinction coefficient for
151 immunoglobulin G (IgG) of 1.36 cm^{-1} (mg · mL^{-1})$^{-1}$ [51]. Assuming a molecular weight of 150,000
152 Da [52], the molar extinction coefficient at 280 nm used for IgG was 210,000 M^{-1} cm^{-1}. The molar
153 extinction coefficient used for α_2-macroglobulin, ε_{280}= 145,440 M^{-1} cm^{-1}, was calculated from
154 amino acid sequence using ProtParam [53].

155 Concentration of Cohn fraction IV was determined using Pierce™ Bicinchoninic Acid (BCA)
156 Protein Assay Kit and bovine serum albumin (BSA) as standard according to the manufacturer's
157 instructions. To calculate a molar concentration, a weighted average protein mass of 80,000 Da
158 was assumed based on the composition of the Cohn fraction IV.

159 **Methylation of proteins**

160 Proteins were dissolved in 1ml 1xPBS pH 7.4 to a concentration of 10 mg · mL^{-1} and the solution
161 cooled to 4 °C. 20 µl of 60 mg · mL^{-1} dimethylamine borane complex and 40 µl 1M
162 formaldehyde were then added. After 2 hours of incubation at 4 °C, this step was repeated. 2
163 hours later a final aliquot of 10 µl dimethylamine borane complex solution was added, before
164 incubation of the reaction mixture at 4 °C overnight. The next morning 125 µl of 1M Tris pH

165 7.5 were added to stop the reaction. The reacting agents were then separated from the now
166 methylated proteins by size-exclusion chromatography using Nap™-5 columns according to
167 the manufacturer's instructions (GE Healthcare Life Sciences, Amersham, UK).

168 **HOCl-treatment of proteins and reduction**

169 The concentration of the NaOCl stock solution of 0.64 M (Sigma-Aldrich, St. Louis, USA) was
170 confirmed regularly by measuring the absorbance at 292 nm using a JASCO V-650 UV/VIS
171 spectrophotometer and the extinction coefficient ε_{292}= 350 M^{-1} cm^{-1}. When necessary, NaOCl
172 stock solution was diluted by mixing an adequate volume of NaOCl with 1x PBS solution pH
173 7.4 immediately prior to each chlorination reaction.

174 Varying amounts of a protein were then treated with a 10-fold, 50-fold and/or 150-fold molar
175 excess of NaOCl for 10 minutes at 30 °C (maximum NaOCl concentration used was 50 mM –
176 a concentration that can be produced by neutrophils per hour in chronically inflamed tissues
177 [31]). Excess HOCl was removed by size-exclusion chromatography using Nap™-5 columns
178 according to the manufacturer's instructions. Due to dilution during the Nap™-5 desalting step,
179 protein concentrations were re-determined as described above.

180 To reverse protein *N*-chlorination in HOCl-treated proteins, sodium ascorbate was dissolved in
181 1xPBS pH 7.4 to a concentration of 1 M and the proteins were incubated with a 50-fold molar
182 excess of sodium ascorbate for 45 minutes at 37 °C. After removal of excess reductant (see
183 above), protein concentrations were again re-determined.

184 **Protein aggregation assays with citrate synthase**

185 200 µL Citrate synthase in ammonium sulfate solution (Sigma-Aldrich, St. Louis, USA) was
186 dialyzed overnight against 2 L 20mM Tris 2mM EDTA buffer at 4°C under constant stirring
187 using a Spectra/Por dialysis membrane with a MWCO of 6-8,000 Da. (Spectrum Laboratories
188 Inc., Rancho Dominguez, CA). This dialyzed citrate synthase preparation was then chemically
189 denatured in 4.5 M GdnHCl, 40 mM HEPES, pH 7.5 at room temperature overnight. The final
190 concentration of denatured citrate synthase was 12 µM. Aggregation was induced by the

191 addition of 20 µL denatured citrate synthase stock to 1580 µL 40 mM HEPES/KOH buffer, pH
192 7.5. Final concentration of citrate synthase in the aggregation assay was thus 0.15 µM.
193 Untreated or treated plasma proteins were added to the assay buffer to a final concentration of
194 0.5 µM (α_2-Macroglobulin) or 1.5 µM (HSA, IgG, γ-globulins, Cohn fraction IV)
195 (corresponding to a 3.3-fold and 10-fold molar excess over the dimeric citrate synthase,
196 respectively) prior to the addition of citrate synthase. The increase of light scattering was
197 monitored in a JASCO FP-8500 fluorescence spectrometer equipped with an EHC-813
198 temperature-controlled sample holder (JASCO, Tokyo, Japan) at 30 °C for 200-240 s under
199 continuous stirring. Measurement parameters were set to 360 nm (Ex/Em), 2.5 nm slit width
200 (Ex/Em) and medium sensitivity. Chaperone activity was expressed as the difference between
201 initial and final light scattering of an individual sample in arbitrary units. Aggregation of citrate
202 synthase in the absence of any other proteins was set to 100%. Depending on the batch of citrate
203 synthase, absolute maximum and minimum light scattering values may vary, thus control
204 experiments with the same batch were carried out for each individual aggregation experiment.

205 **Detection of accessible amino groups in proteins**

206 Accessible amino groups in HSA were detected using fluorescamine (Sigma-Aldrich, St. Louis,
207 USA) as described [54]. Briefly, 334 µl of 3 mg · mL^{-1} fluorescamine stock in acetone were added
208 to 1 mL of 80 µg · mL^{-1} native HSA or the variously treated HSA solutions described above.
209 Emission spectrum of fluorescamine from 400 to 600 nm was measured upon excitation with
210 388 nm using a JASCO FP-8500 fluorescence spectrometer. The relative amount of accessible
211 amino groups in the variously treated HSA samples was calculated by setting the maximum
212 fluorescence of native HSA to 100% representing the total relative amino group content.

213 **Nile red hydrophobicity assay**

214 Nile red (Sigma-Aldrich, St. Louis, USA) was dissolved in dimethyl sulfoxide (DMSO) to a
215 final concentration of 30 µM. Varying amounts of native or HOCl-treated HSA (0-200 µM) in
216 1xPBS were mixed with Nile red stock to a final dye concentration of 1.6 µM. Fluorescence

217 was measured using a JASCO FP-8500 fluorescence spectrometer with the following
218 parameters: 550 nm excitation, 570-700 nm emission, 5 nm slit width (Ex/Em) and medium
219 sensitivity. Concentrations of native or HOCl-treated HSA, at which the proteins were half-
220 saturated with dye were calculated by plotting the fluorescence intensity of Nile red against the
221 logarithm of the molar protein concentrations. Data were fitted with GraphPad Prism 8 software
222 using the sigmoid fit function.

223 **PLB-985 culture and differentiation**

224 The human myeloid leukemia cell line PLB-985 (certified mycoplasma negative, obtained from
225 DSMZ, German collection of microorganisms and cell culture) was cultured in RPMI-1640
226 medium supplemented with 10% heat-inactivated FBS and 1% GlutaMAX (Life Technologies,
227 Carlsbad, CA) at 37°C with 5% CO_2. Cells were passaged twice weekly to maintain a cell
228 density between 2×10^5 and $1 \times 10^6 \cdot mL^{-1}$ and used until passage no. 10. For differentiation
229 into neutrophil-like cells, cells were seeded at a density of $2 \times 10^5 \cdot mL^{-1}$ and cultured for 96
230 hours in RPMI-1640 medium with 10% FBS, 1% GlutaMAX and 1.25% DMSO [55]. After 72
231 hours of incubation in the presence of DMSO, 2000 $U \cdot mL^{-1}$ interferon-γ (ImmunoTools,
232 Friesoythe, Germany) was added to the cell culture [56]. In a previous study, differentiation was
233 checked by detecting the expression of the associated surface markers CD11b and CD64 (see
234 ref. [7]). The viability of the cells was evaluated using trypan blue dye and was typically >90%.

235 **Chemiluminescence-based NADPH-oxidase activity assay**

236 NADPH-oxidase-dependent superoxide production was selectively measured by
237 chemiluminescence (CL) using the chemiluminogenic substrate lucigenin (10,10'-Dimethyl-
238 9,9'-biacridinium dinitrate; Carl Roth, Karlsruhe, Germany) [57].

239 Differentiated PLB-985 cells were washed once with 1xPBS pH 7.4 and diluted in the same
240 buffer to a final concentration of 5×10^6 cells $\cdot mL^{-1}$. 100 µL of this cell suspension were placed
241 in the wells of a non-transparent, white, clear-bottom 96-well plate (Nunc, Rochester, NY). For
242 some experiments, cells were preincubated with 10 µM diphenyleneiodium (DPI; NADPH

243 oxidase inhibitor), 100 nM wortmannin (phosphoinositide 3-kinase (PI3K) inhibitor), 200 nM
244 Gö 6983 (protein kinase C (PKC) inhibitor) or vehicle (1% DMSO) for 30 minutes at 37 °C.
245 All inhibitors dissolved in DMSO were purchased from Sigma-Aldrich, St. Louis, USA. The
246 final concentration of DMSO in all wells was adjusted to 1%. The bottom of the plate was
247 covered using a white, non-transparent adhesive seal prior to measurement. 50 µL of either
248 1xPBS (resting CL) or agents to be tested, including the untreated and treated plasma proteins
249 were added to the respective wells. Final concentrations were: 2 mg · mL^{-1} α_2-macroglobulin,
250 3 mg · mL^{-1} HSA, IgG, γ-globulins and Cohn fraction IV, 0.2 µM PMA (Phorbol 12-myristate
251 13-acetate; Sigma-Aldrich, St. Louis, USA). Lucigenin was dissolved in 1xPBS to a
252 concentration of 400 µM immediately prior to measurement and 50 µL were added to the wells.
253 Chemiluminescence was measured every 1-2 minutes over 1.5 hours at 37 °C using the Synergy
254 H1 multi-detection microplate reader (Biotek, Bad Friedrichshall, Germany) in triplicates and
255 chemiluminescence activity was expressed as integrated total counts as calculated by the
256 addition of rectangles with unit width under individual data points. In inhibition assays,
257 NADPH-oxidase activation, as measured by chemiluminescence activity, induced by PMA,
258 HSA, treated with a 50-fold molar excess of HOCl, or IgG, treated with a 150-fold molar excess
259 of HOCl, was set to 100% and other relevant data as percentage of this control.

260 **Cloning of Ag85B**

261 *E. coli* strains, plasmids and primers used in this study are listed in Table 1. Ag85B gene (*fbpB*)
262 of *Mycobacterium bovis* (differs by one base-pair from corresponding gene of *M. tuberculosis*,
263 resulting in a Leu to Phe replacement at position 100 [58]) was designed with optimized codon
264 usage for expression in *E. coli*, synthesized and cloned into pEX-A2 standard vector by
265 Eurofins Genomics. *fbpB* was amplified from pEXA_fbpB by PCR using primers fbpB-fw and
266 fbpB-rv, purified according to the instructions of the NucleoSpin Gel and PCR Clean-up Kit
267 (Macherey-Nagel GmbH, Düren, Germany) and cloned into the pET22b(+) expression vector
268 via the restriction sites NdeI and XhoI with a hexahistidine (His_6)-tag placed at the C-terminal

269 end of the gene. *E. coli* DH5α cells were transformed with the plasmid using a standard heat-
270 shock method and plated on Luria Bertani (LB) agar plates supplemented with 50 μg · mL^{-1}
271 ampicillin. Screening for recombinant plasmids was performed by colony PCR, followed by
272 isolation of potentially correct plasmids from the respective strains. Successful cloning of *fbpB*
273 gene into pET22b(+) vector was verified by sequencing.

274 **Table 1: *E. coli* strains, plasmids and primers used in this study.**

	Relevant properties [a] or genotype	Source or reference
***E. coli* strains**		
DH5α	*supE44, ΔlacU169* (*φ80 lacZΔM15*) *hsdR17 recA1 endA1 hsdR gyrA relA thi*	Invitrogen
BL21(DE3)	*F⁻ ompT gal dcm lon hsdS$_B$(r$_B^-$ m$_B^-$) λ(DE3 [lacI lacUV5- T7 gene 1 ind1 sam7 nin5])*	Stratagene, Santa Clara, CA
Plasmids		
pEXA_fbpB	Amp^R pEX-A128 vector carrying synthesized *fbpB* gene from *M. bovis*	Eurofins Genomics
pET22b (+)	Amp^R, vector for overexpression of genes in *E. coli*	Novagen
pET22b-fbpB	Amp^R, vector for overexpression of *fbpB* gene in *E. coli* BL21(DE3)	This study
Primers	**Sequence (5' -> 3')**	
fbpB-fw	CCCCATATGTTCTCTCGTCCGG	
fbpB-rv	CCCCTCGAGACCAGCACCCAG	

275 [a] Amp^R, ampicillin resistance

276 **Expression and purification of Ag85B**

277 For heterologous expression and subsequent purification of His$_6$-tagged Ag85B, recombinant
278 plasmid pET22b-fbpB was transferred into the *E. coli* expression strain BL21 (DE3) (see
279 Table 1). The transformed cells were plated on LB agar plates containing 50 µg · mL^{-1}
280 ampicillin and incubated at 37 °C for 24 hours. 2 x 50 ml LB medium with ampicillin were
281 inoculated with a single colony from the agar plate and incubated at 37 °C overnight. These
282 overnight cultures were then used for inoculation of 5 x 1 L ampicillin-containing LB medium
283 to a starting optical density at 600 nm (OD$_{600}$) of 0.1. The bacteria were grown at 37 °C with
284 shaking at 130 rpm until the OD$_{600}$ was ~ 0.5. Expression of Ag85B including a C-terminal
285 hexahistidine (His$_6$)-tag was induced with 1 mM isopropyl-beta-D-thiogalactopyranoside
286 (IPTG) and continued for ~ 12 hours (overnight) at 20 °C. Cells were harvested by
287 centrifugation at 6500 x g for 45 minutes at 4 °C. Pellets were washed once with 1xPBS and
288 resuspended in lysis buffer (5 mM imidazole, 300 mM NaCl, 50 mM NaH_2PO_4, pH 8.0). Cells

289 were disrupted using a Constant Cell disrupter (Constant Systems Limited, Daventry, England),
290 and the obtained lysate was centrifuged for 45 minutes at 4 °C and 57,500 x g. Solid precipitate
291 and the supernatant were separated and evaluated for detection of recombinant protein by SDS-
292 PAGE, followed by Coomassie Blue G-250 staining. Overexpressed Ag85B protein was found
293 predominantly in the pellet fraction. Pellet was thus resuspended in lysis buffer containing 8 M
294 urea and thoroughly homogenized. Suspension was applied to a polystyrene column filled with
295 nickel-nitrilotriacetic (Ni-NTA) resin, and washed with urea-containing lysis buffer, followed
296 by a washing step with wash buffer supplemented with a small amount of imidazole (8M urea,
297 20 mM imidazole, 300 mM NaCl, 50 mM NaH_2PO_4, pH 8.0). Recombinant Ag85B was eluted
298 from the column using 250 mM imidazole buffer solution (8M urea, 250 mM imidazole, 300
299 mM NaCl, 50 mM NaH_2PO_4, pH 8.0). In order to remove imidazole, combined elution fraction
300 was diluted 1:10 in sodium phosphate buffer (300 mM NaCl, 50 mM NaH_2PO_4, pH 8.0) and
301 mixed overnight at 4 °C. Precipitated protein was collected by centrifugation for 45 minutes at
302 4 °C and 57,500 x g and resuspended in urea-containing sodium phosphate buffer (8M urea,
303 300 mM NaCl, 50 mM NaH_2PO_4, pH 8.0). Concentration of purified Ag85B protein was
304 quantified spectrophotometrically by measuring the absorbance at 280 nm using a JASCO V-
305 650 UV/VIS spectrophotometer. The molar extinction coefficient used for Ag85B was ε_{280}=
306 75,860 M^{-1} cm^{-1} [59].

307 **Flow cytometry-based cell apoptosis assay**

308 Differentiated PLB-985 cells were counted, washed once with 1xPBS pH 7.4 and diluted in
309 RPMI-1640 medium supplemented with 10% heat-inactivated FBS to a final concentration of
310 3.3×10^6 cells · mL^{-1}. 600 µL of this cell suspension were placed in the wells of a transparent,
311 flat-bottom 24-well plate (Sarstedt, Nümbrecht, Germany). The cells were preincubated with
312 100 nM wortmannin, 50 µM Z-VAD-FMK, a broad spectrum pan-caspase inhibitor (dissolved
313 in DMSO; Santa Cruz Biotechnology, Dallas, TX, USA), 250 µM cytochalasin D, an inhibitor
314 of actin polymerization (dissolved in DMSO; Sigma-Aldrich, St. Louis, USA), 155 µM native

315 or modified HSA, that has been treated with a 50-fold molar excess of HOCl as described above,
316 or vehicle (1% DMSO) for 1 hour at 37 °C. The final concentration of DMSO in all wells was
317 adjusted to 1%. Subsequently, 1 µM Ag85B (85 µM stock in urea-containing buffer (8 M urea,
318 300 mM NaCl, 50 mM NaH_2PO_4, pH 8.0)), 2 µM staurosporine (dissolved in DMSO; Sigma-
319 Aldrich, St. Louis, USA) or vehicle (94 mM urea and 1% DMSO) were added. After 1 hour of
320 incubation with Ag85B or 6 hours with staurosporine at 37°C, cells were washed once with
321 cold 1xPBS, followed by one washing step with 1x Annexin V binding buffer. For the analysis
322 of cell viability, the variously treated cell suspensions were stained with Annexin V-FITC and
323 propidium iodide (PI) using the Dead Cell Apoptosis Kit (Invitrogen, Thermo Fisher Scientific,
324 Waltham, Massachusetts, USA) according to the manufacturer's instructions and subsequently
325 subjected to flow cytometry. Samples were analyzed using a BD FACSCanto II flow cytometer
326 (Becton, Dickinson and Company). Fluorescence emitted by Annexin V-FITC and PI was
327 measured through a 530/30-nm and 585/42-nm bandpass filter, respectively, upon excitation
328 with an argon ion laser operating at 488 nm. Single-stained compensation controls were used
329 to calculate the compensation matrix. 20,000 events were acquired and recorded per sample.
330 Data were analyzed using FlowJo (version 10) software.

331 **Fluorescent labeling of Ag85B**

332 For fluorescent labeling of Ag85B the green fluorescent dye CF^{TM} 488A succinimidyl ester
333 (Sigma-Aldrich, St. Louis, USA) was used. Labeling occurred via reaction of the succinimidyl
334 ester group of the dye with amine groups of Ag85B. Labeling was performed according to the
335 manufacturer's instructions with slight modifications. To prevent aggregation of Ag85B,
336 labeling reaction was performed in urea-containing buffer (8 M urea, 300 mM NaCl, 50 mM
337 NaH_2PO_4, pH 8.0) and carried out for 6 hours at room temperature under continuous shaking.
338 Excess dye was removed by size-exclusion chromatography using PD-10 desalting columns
339 containing Sephadex G-25 resin according to the manufacturer's instructions (GE Healthcare

340 Life Sciences, Amersham, UK). Concentration of the conjugate and degree of labeling (DOL)
341 were calculated using the formula provided by the dye's manufacturer. DOL was 3.1.

342 **Ag85B-488 uptake assay**

343 For the antigen uptake assay, differentiated PLB-985 cells were incubated with fluorescently-
344 labeled Ag85B (Ag85B-488) protein in the presence or absence of native and HOCl-modified
345 HSA in the same way as for the cell apoptosis assay described above. After 1 hour of incubation
346 at 37°C, cells were washed twice with 1xPBS, followed by fixation with 4% paraformaldehyde
347 (PFA) for 10 minutes on ice. Cells were washed with 1xPBS and subsequently subjected to
348 flow cytometry. Samples were analyzed using a BD FACSCanto II flow cytometer.
349 Fluorescence emitted by Ag85B-488 was measured through a 530/30-nm bandpass filter upon
350 excitation with the 488 nm argon laser line. 30,000 events were acquired and recorded per
351 sample. Data were analyzed using FlowJo (version 10) software.

352 **Ag85B aggregation assay**

353 Aggregation of Ag85B was induced by the stepwise addition of 75 µL Ag85B stock (5 x 15 µL
354 every 20 seconds) to 1525 µl 40 mM HEPES/KOH buffer, pH 7.5. Final concentration of
355 Ag85B in the aggregation assay was 0.186 µM. Native or variously treated HSA as described
356 above, was added to the assay buffer to a final concentration of 14.88 µM (corresponding to a
357 80-fold molar excess over Ag85B) prior to the addition of Ag85B. The increase of light
358 scattering was monitored in a JASCO FP-8500 fluorescence spectrometer equipped with an
359 EHC-813 temperature-controlled sample holder at 30 °C for 200 s under continuous stirring.
360 Measurement parameters were set to 360 nm (Ex/Em), 2.5 nm slit width (Ex/Em) and medium
361 sensitivity. Chaperone activity was expressed as the difference between initial and final light
362 scattering of an individual sample in arbitrary units. Aggregation of Ag85B in the absence of
363 HSA was set to 100%.

364 **RESULTS**

365 **HOCl-treated human serum prevents protein aggregation**

366 In previous experiments we showed that the bacterial protein RidA is transformed into a
367 competent holdase-type chaperone upon treatment with HOCl or *N*-chloramine [17]. In control
368 experiments, we discovered that bovine serum albumin also shows increased chaperone activity
369 in response to HOCl [17]. Since HOCl can be present in a physio-pathological context, most
370 notably in the vicinity of inflammation, we wanted to test if human serum proteins can also be
371 transformed into holdase-type chaperones through HOCl-treatment. Thus, we performed
372 aggregation assays using chemically denatured citrate synthase and untreated and HOCl-treated
373 human serum. Human serum was incubated with an estimated 10-fold molar excess of HOCl
374 for 10 minutes at 30°C, a concentration that was sufficient to fully activate or markedly improve
375 the chaperone function of RidA and BSA, respectively [17]. When chemically denatured citrate
376 synthase was diluted into denaturant-free buffer, it formed aggregates that can be monitored by
377 increased light scattering of the solution (Fig. 1). This aggregation of citrate synthase was not
378 prevented by the addition of untreated human serum. However, when pre-incubated with a 10-
379 fold molar excess of HOCl, serum significantly decreased aggregate formation. This suggested
380 to us, that at least some serum proteins could be transformed to a holdase-type chaperone by *N*-
381 chlorination in a mechanism similar to RidA. Because *N*-chlorination can be reduced by certain
382 antioxidants, we used ascorbate to re-reduce HOCl-treated serum. Ascorbate is a mild
383 antioxidant, which typically does not reduce native or HOCl-induced disulfide bonds. This
384 ascorbate-treated serum lost its capability to bind denatured citrate synthase, suggesting an *N*-
385 chlorination-based mechanism.

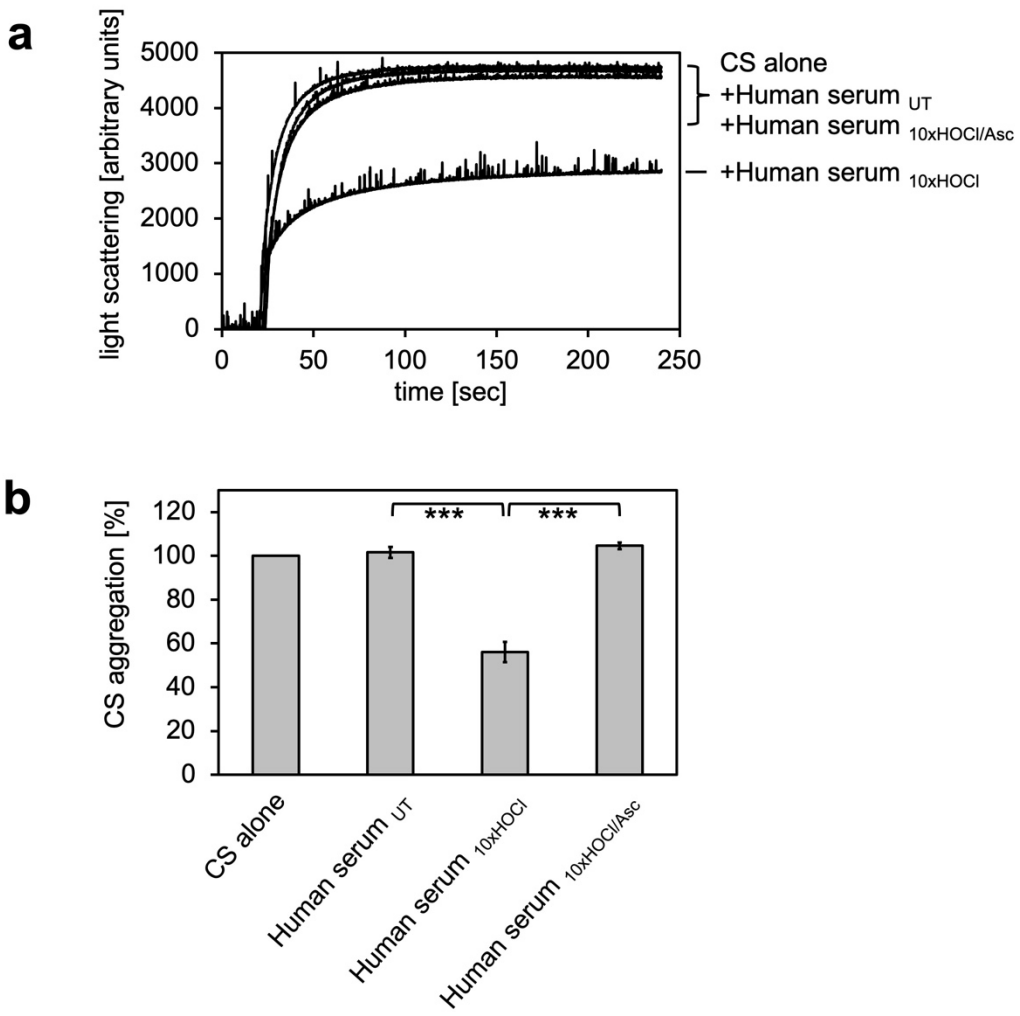

Figure 1: HOCl-treated human serum decreases protein aggregation. Human serum, when treated with a 10-fold molar excess of HOCl (Human serum $_{10xHOCl}$), significantly decreases aggregation of chemically-denatured citrate synthase as measured by light scattering at 360 nm. Reduction of HOCl-treated human serum with a 50-fold molar excess of the antioxidant ascorbate (Human serum $_{10xHOCl/Asc}$) reverses this chaperone-like conversion of the serum. **(a)** A representative measurement of citrate synthase aggregation in the presence of untreated (Human serum $_{UT}$), HOCl-treated (Human serum $_{10xHOCl}$) and re-reduced (Human serum $_{10xHOCl/Asc}$) human serum is shown. **(b)** Data are represented as means and standard deviations from three independent aggregation assays. Student's t-test: ***$p < 0.001$. Aggregation of citrate synthase in the absence of human serum was set to 100% and all the data are presented as percentage of this control. Labels of aggregation curves are written in the order of the final intensity of light scattering of the respective treatment.

Albumin, the major protein component of serum, shows HOCl-induced chaperone-like activity

The major protein component of human serum is human serum albumin (HSA). Previously, we showed that its bovine homologue bovine serum albumin (BSA) exhibits increased chaperone activity upon treatment with HOCl [17]. We therefore suspected that HSA could be a major

402 contributor to the observed decrease in protein aggregate formation in the presence of HOCl-
403 treated serum. To test whether HSA gains chaperone function upon exposure to HOCl, HSA at
404 a final concentration of 1 mM was treated with a 10-fold molar excess of HOCl for 10 minutes
405 at 30 °C. An HOCl concentration of at least 10 mM has been shown to be required for the
406 generation of significant quantities of the so-called advanced oxidation protein products
407 (AOPPs) in plasma, associated with a number of inflammatory diseases [41]. The localized
408 concentration of HOCl generated by accumulated neutrophils in the interstitium of chronically
409 inflamed tissues, however, can be much higher and reach values of 25-50 mM per hour [31]. To
410 mimic a state of chronic inflammation, HSA was thus also incubated in the presence of a 50-
411 fold molar excess of HOCl corresponding to the maximum reported concentration of 50 mM.
412 HSA treated in both ways significantly reduced the aggregation of citrate synthase when added
413 at a 10-fold molar excess, showing that HSA acts as a potent chaperone in serum upon
414 modification by HOCl (Fig. 2 a, b). The chaperone activity of HSA, however, was much higher
415 upon exposure to a 50-fold molar excess of HOCl, suggesting a dose-dependent activation of
416 the HSA chaperone function by HOCl. In contrast to bacterial RidA and Hsp33 [17,19], full
417 activation of the chaperone function of HSA seems to require a higher oxidation/chlorination
418 level of the protein.

419 **Chaperone-like conversion of serum albumin can be reversed by antioxidants**

420 It is well known that exposure to high HOCl concentrations, such as those present at sites of
421 chronic inflammation, can lead to plasma protein unfolding and the formation of carbonylated
422 and di-tyrosine cross-linked protein aggregates that cannot return to the free, functional pool of
423 proteins upon reduction by antioxidants [16]. Such irreversibly misfolded plasma proteins could
424 principally act as chaperones and bind to and prevent the aggregation of other unfolding
425 substrates through hydrophobic interactions with the newly exposed hydrophobic protein
426 surfaces.

427 However, based on the observation that the chaperone activity of serum albumin increased in a
428 dose-dependent manner with the quantity of HOCl added, we asked whether the activation of
429 HSA chaperone function upon treatment with a 10- or 50-fold molar excess of HOCl could be
430 mediated by reversible *N*-chlorination instead. We have found this mechanism of action in the
431 bacterial protein RidA [17]. We thus exposed HOCl-treated HSA to a 50-fold molar excess of the
432 antioxidant ascorbate, which specifically removes *N*-chlorination. Indeed, ascorbate rendered
433 $HSA_{10xHOCl}$ and $HSA_{50xHOCl}$ unable to prevent citrate synthase aggregation when added at the
434 same molar excess as the HOCl-treated protein samples (Fig. 2 c, d). This result strongly
435 supports the idea that HOCl-mediated activation of HSA chaperone function involves
436 reversible chlorination of its side chain amines.

437 **Methylation of basic amino acid residues in serum albumin inhibits HOCl-induced**
438 **activation of its chaperone function**

439 Prompted by the observation that HOCl-mediated conversion of serum albumin into a potent
440 chaperone could be reversed by ascorbate, we assumed an *N*-chlorination-based activation
441 mechanism of its chaperone function. To further confirm this hypothesis, we blocked free
442 amino groups of lysine and nitrogens in the guanidino-moiety of arginine residues in HSA via
443 selective methylation. Exposure of methylated HSA to 10- or 50-fold molar excess of HOCl
444 did not convert HSA into a chaperone, suggesting that activation of the HSA chaperone function
445 indeed requires chlorination of its basic amino acids (Fig. 2 e, f).

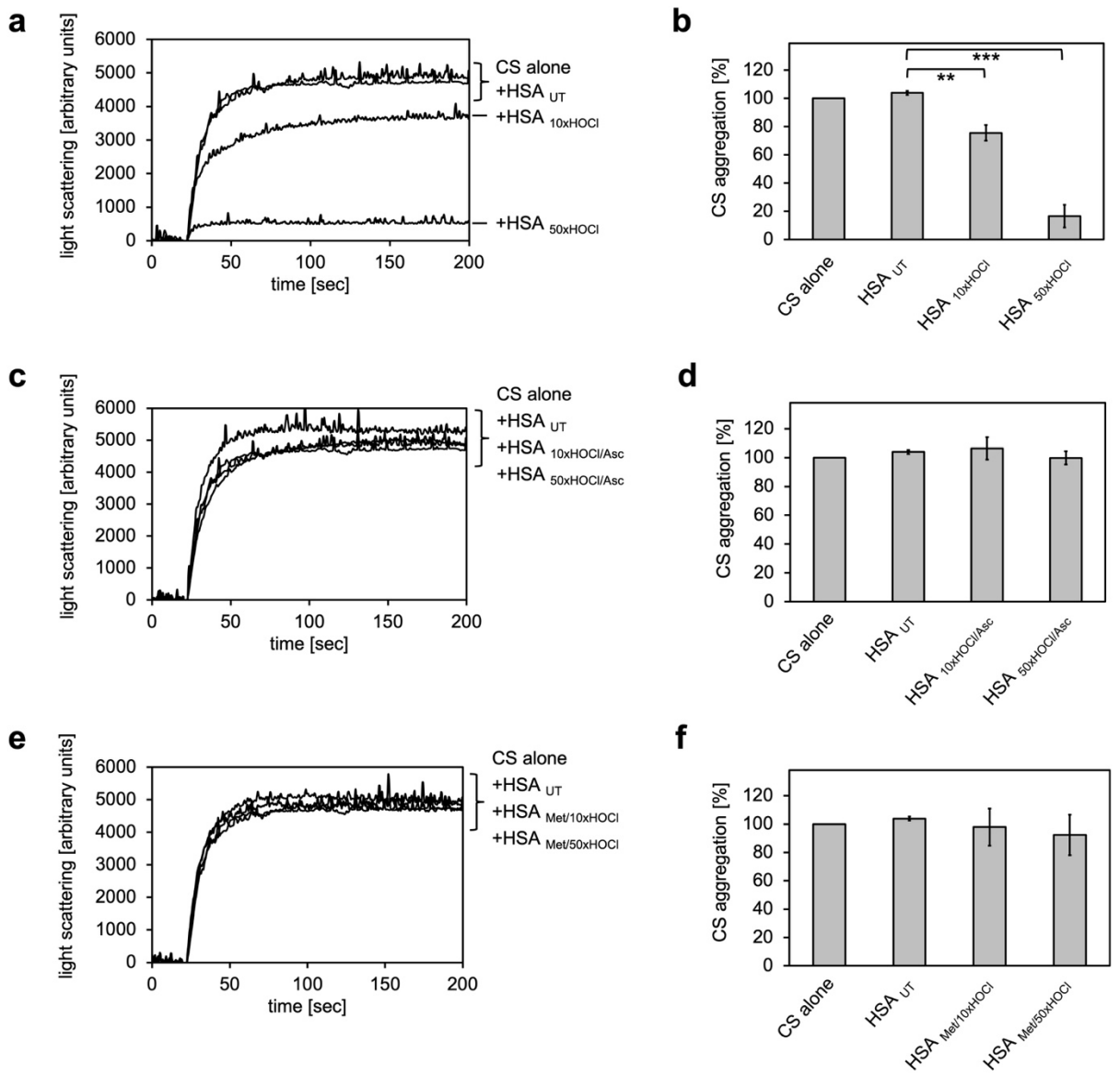

Figure 2: Conversion of serum albumin into a potent chaperone upon HOCl exposure is based on reversible *N*-chlorination of its basic amino acids. (a, b) Serum albumin, when treated with a 10- or 50-fold molar excess of HOCl ($HSA_{10xHOCl}$ and $HSA_{50xHOCl}$, respectively), significantly decreases aggregation of chemically-denatured citrate synthase as measured by light scattering at 360 nm. **(c, d)** Reduction of HOCl-treated HSA with a 50-fold molar excess of the antioxidant ascorbate ($HSA_{10xHOCl/Asc}$ and $HSA_{50xHOCl/Asc}$) switches off its chaperone activity. **(d, e)** Methylation of basic amino acid side chains prior to HOCl treatment ($HSA_{Met/10xHOCl}$ and $HSA_{Met/50xHOCl}$) abrogates the chaperone-like conversion of HSA. In **a**, **c** and **e** representative measurements are shown. In **b, d** and **f** data are represented as means and standard deviations from three independent experiments. Student's t-test: $^{**}p < 0.01$, $^{***}p < 0.001$. Aggregation of citrate synthase in the absence of HSA was set to 100% and all the data are presented as percentage of this control. Labels of aggregation curves are written in the order of the final intensity of light scattering of the respective treatment.

459 **Decreased amino group content of HSA upon HOCl treatment is accompanied by an**
460 **increased overall hydrophobicity of the protein**

461 Our combined data strongly suggested that the chaperone function of HSA is activated by
462 chlorination of its basic amino acids. HSA in its secreted form possesses 84 potential targets
463 for chlorination by HOCl: 59 lysine residues, 24 arginine residues and one amino group at the
464 N-terminus [60]. To investigate the extent to which HOCl decreases the total amount of
465 accessible, non-modified amino groups in HSA, we analyzed the free amino group content
466 before and after HOCl-treatment using fluorescamine [54]. Evidently, exposure to HOCl resulted
467 in some loss of free amino groups. Amino group content of HSA decreased by approximately
468 10% after treatment with a 10-fold molar excess of HOCl ($HSA_{10xHOCl}$) and by 40% upon
469 exposure to a 50-fold molar excess of HOCl ($HSA_{50xHOCl}$) (Fig. 3 a, b). Reduction of both
470 chlorinated HSA samples with ascorbate resulted in a full recovery of accessible amino groups
471 with concomitant loss of chaperone activity (Fig. 2 c, d). Activation of HSA chaperone function
472 by HOCl thus coincides with a decrease in free amino group content, providing further evidence
473 for an *N*-chlorination based-mechanism.

474 We argued that the reduction of positive charges on the protein's surface through HOCl-induced
475 *N*-chlorination should lead to an increase in surface hydrophobicity, thus allowing high-affinity
476 binding to unfolded proteins.

477 To detect changes in HSA's surface hydrophobicity upon HOCl treatment, we used the
478 uncharged hydrophobic dye Nile red and measured its fluorescence upon addition to 25 µM
479 native HSA or 25 µM $HSA_{50xHOCl}$ [61]. Absolute fluorescence of 1.6 µM Nile red was higher for
480 $HSA_{50xHOCl}$ when compared with untreated HSA with a maximum at 616.5 nm (621.5 nm for
481 native HSA) showing a blue shift in emission maximum consistent with a decreased polarity of
482 the protein solution (Fig. 3 c). The concentration of native HSA and $HSA_{50xHOCl}$, at which the
483 proteins have been half-saturated with dye were calculated (Fig. 3 d). This concentration was

484 significantly higher for untreated HSA compared to $HSA_{50xHOCl}$, pointing towards an increased
485 hydrophobicity of $HSA_{50xHOCl}$.
486

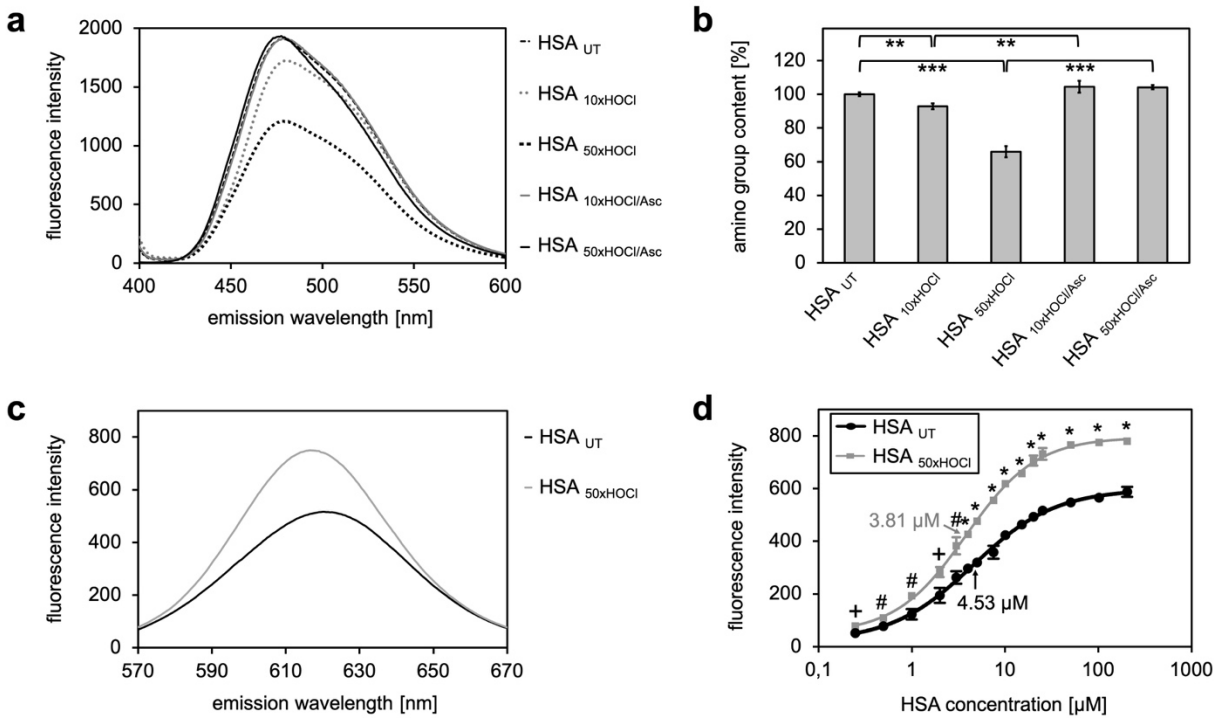

487

488 **Figure 3: *N*-chlorination of serum albumin decreases accessible amino group content and increases surface**
489 **hydrophobicity.** (**a**, **b**) Amino group content of variously treated HSA was analyzed using fluorescamine.
490 Treatment of HSA with HOCl resulted in a dose-dependent loss of free amino groups. Reduction of chlorinated
491 HSA with ascorbate fully restored the free amino group content. (**c**) Fluorescence of 1.6 µM Nile red in the
492 presence of native HSA or HSA, that has been treated with a 50-fold molar excess of HOCl. An increased absolute
493 fluorescence and a shift in maximum emission wavelength (from 621.5 nm to 616.5 nm) can be observed for
494 $HSA_{50xHOCl}$. (**d**) Absolute fluorescence of Nile red measured at the emission maximum at 621.5 nm and 616.5 nm,
495 respectively, was plotted against the corresponding HSA_{ut} and $HSA_{50xHOCl}$ concentrations, respectively. The
496 average concentrations, at which HSA_{ut} and $HSA_{50xHOCl}$ have been half-saturated with Nile red are marked by
497 arrows. Means and standard deviations in **b** and **d** are based on three independent experiments. (**b**) Student's t-
498 test: $*p < 0.05$, $**p < 0.01$, $***p < 0.001$. (**d**) Student's t-test: $^{+}p < 0.05$, $^{\#}p < 0.01$, $*p < 0.001$. For **a** and **c**
499 representative measurements are shown.

500 **Activation of neutrophil-like cells by HOCl-treated serum albumin is based on reversible**
501 ***N*-chlorination**

502 Several lines of evidence point toward a key role of HOCl-modified serum albumin in the
503 progression of chronic inflammation, a hallmark of various degenerative diseases [46,47]. Upon

504 exposure to high doses of HOCl, as those present in chronically inflamed tissues, modified HSA
505 was found to induce neutrophil NADPH oxidase activation reflected by an increased generation
506 of reactive oxygen species and accompanied by degranulation [47].
507 Pathophysiological concentrations of HOCl are able to induce different modifications on
508 plasma proteins including carbonylation, *N*-chlorination, cysteine and methionine oxidation or
509 inter- and intramolecular di-tyrosine cross-linking [8,9,11,16], with most of them being considered
510 irreversible. So far, it has not been elucidated which HOCl-induced modification is sufficient
511 to convert HSA into a potent activator of leukocytes. We thus wondered whether this functional
512 conversion of HSA might be specifically mediated by *N*-chlorination and thus reflects a
513 reversible process, similar to the activation of its chaperone function in response to HOCl stress.
514 To test this, we analyzed the effect of HOCl-treated HSA before and after reduction by
515 antioxidants on the activity of the phagocytic NADPH oxidase. For this purpose, we chose the
516 human myeloid cell line PLB-985 that acquires a neutrophil-like phenotype upon
517 differentiation with DMSO and IFNγ [55,56].
518 Generation of oxidants by the NADPH oxidase was assessed by lucigenin, a well characterized
519 and frequently used chemiluminescence probe which predominantly reacts with superoxide
520 anion radicals to form a light-emitting species [62]. Differentiated PLB-985 cells, when incubated
521 in buffer in the absence of any activating agents, showed a low basal level of superoxide
522 generation resulting from IFNγ-mediated enhancement of the NADPH oxidase activity during
523 the differentiation period [63] (Fig. 4 a). In line with expectations, treatment of the cells with
524 phorbol-12-myristate-13-acetate (PMA), a known activator of neutrophil NADPH oxidase, led
525 to a drastic increase in superoxide production and was thus used as positive control [64] (Fig. 4 a,
526 c). Addition of untreated HSA significantly increased the generation of superoxide by > 20%
527 compared to the mock control. No further enhancement of the NADPH oxidase activity was
528 observed with HSA after exposure to a 10-fold molar excess of HOCl, indicating that the chosen
529 HOCl concentration might have been too low for the conversion of HSA into a potent activator

530 of neutrophil-like cells. In contrast, cells subjected to HSA that has been treated with a 50-fold
531 molar excess of HOCl exhibited a substantial increase in superoxide production within the first
532 ~ 25 minutes of incubation. In comparison to PMA, NADPH oxidase activation by $HSA_{50xHOCl}$
533 proceeded at a lower rate and was less sustained, returning to basal level 40 minutes after the
534 addition of $HSA_{50xHOCl}$ to the cells.
535 During our experiments we observed that *N*-chlorinated HSA can directly react with the
536 fluorescent dye, 2', 7'-dichlorodihydrofluorescein diacetate (H_2DCF-DA), which is the most
537 widely used probe for measuring intracellular ROS production [65], eliciting a positive signal in
538 the absence of cells (Supplementary Fig. S1). To confirm that the observed chemiluminescent
539 signal emitted by lucigenin derives from $HSA_{50xHOCl}$-induced activation of the phagocytic
540 NADPH-oxidase rather than from a similar direct reaction of lucigenin with $HSA_{50xHOCl}$ -
541 derived chloramines, we incubated lucigenin with the various agents in the absence of cells and
542 no significant chemiluminescence was observed (Fig. 4 b).
543 Importantly, when reduced by ascorbate, $HSA_{50xHOCl}$ lost its stimulatory effect, showing that
544 the functional conversion of HSA to an efficient activator of neutrophil-like cells upon HOCl
545 exposure reflects a reversible process. Since ascorbate specifically reduces *N*-chloramines
546 without affecting other HOCl-induced modifications, these results strongly support an *N*-
547 chlorination-based mechanism. The latter finding was further corroborated by methylation of
548 the basic amino acids of HSA prior to HOCl treatment, which completely prevented HOCl-
549 treated HSA from activating the neutrophil oxidative burst.
550 *N*-chlorinated HSA, formed upon exposure to high doses of HOCl, can be thus considered as
551 an inflammatory response modulator that contributes to the activation of neutrophils at sites of
552 inflammation.

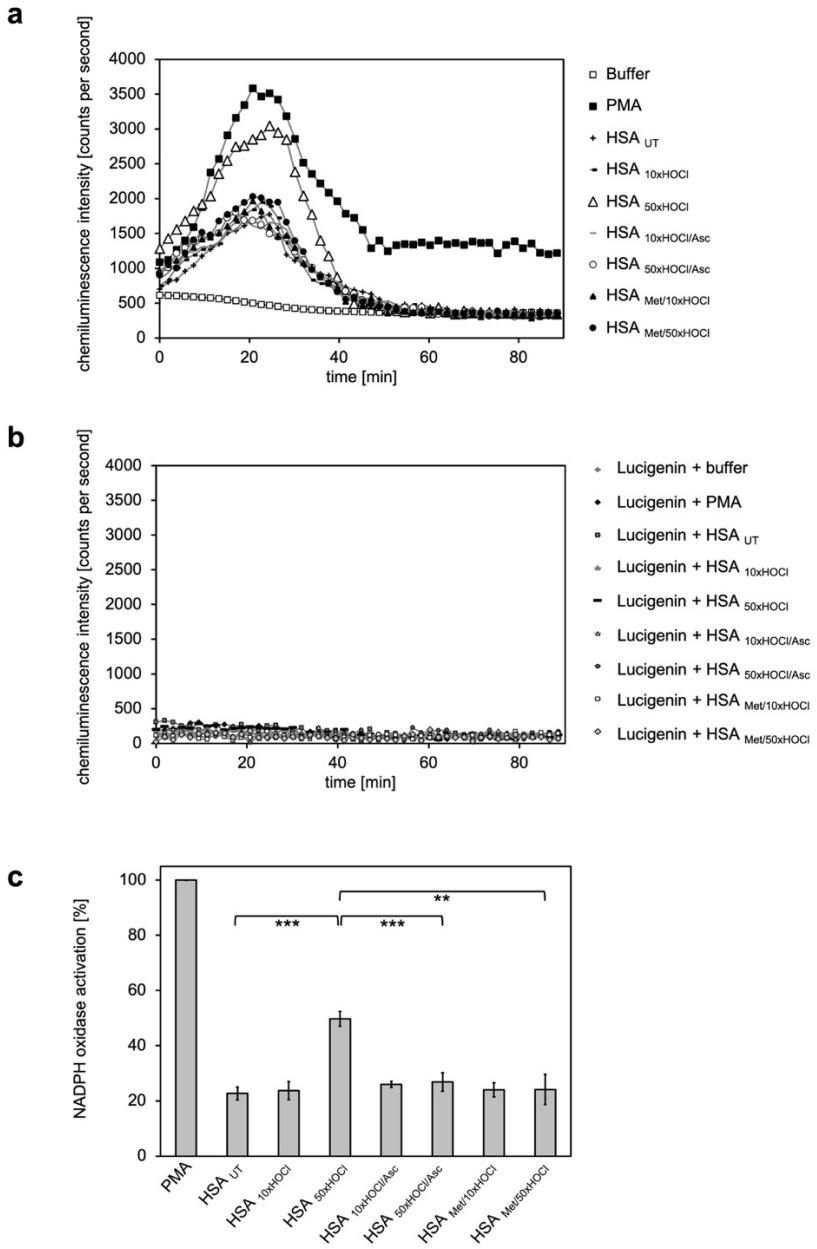

Figure 4: Activation of neutrophil-like cells by HOCl-treated serum albumin is mediated by reversible *N*-chlorination. Treatment with a 50-fold molar excess of HOCl (HSA $_{50xHOCl}$) converted HSA into an efficient inducer of the neutrophil respiratory burst, reflected by the increased production and release of oxidants that induce lucigenin chemiluminescence. This activating function of HSA $_{50xHOCl}$ could be reversed by reduction with the antioxidant ascorbate (HSA $_{50xHOCl/Asc}$) and was abrogated by methylation of its basic amino acid side chains prior to HOCl exposure (HSA $_{Met/50xHOCl}$). **(a)** Extracellular oxidant production by neutrophil NADPH oxidase was measured in one- to two-minutes intervals over 90 minutes at 37 °C using lucigenin-enhanced chemiluminescence. Phorbol 12-myristate 13-acetate (PMA; final concentration, 0.2 µM), untreated and variously treated HSA samples (final concentration, 3 mg · mL^{-1}) from the previous citrate synthase aggregation assays (see above) or PBS buffer (basal oxidant production) were added to **(a)** differentiated PLB-985 cells in PBS buffer or **(b)** cell-free PBS puffer containing 400 µM lucigenin immediately prior to chemiluminescence measurement. **(c)** Results shown in **a** are expressed as integrated total counts (means and standard deviations of three independent measurements) higher

566 than buffer control. Student's t-test: **$p < 0.01$, ***$p < 0.001$. PMA-induced activation of NADPH-oxidase was
567 set to 100%.

568 **All plasma fractions tested exhibit chaperone activity upon HOCl treatment**

569 Our finding that the major protein in human plasma, serum albumin. can be converted into a
570 potent chaperone upon HOCl-mediated *N*-chlorination, prompted us to ask whether also other
571 plasma protein fractions exhibit similar chaperone activity upon treatment with HOCl.

572 We thus tested the γ-globulin fraction, the Cohn fraction IV (comprising α- and β-globulins),
573 and specifically α_2-macroglobulin, an important protease inhibitor in human plasma, for
574 chaperone activity upon exposure to various doses of HOCl.

575 Aside from its known interaction with proteases, native α_2-macroglobulin (α_2M) acts as an
576 extracellular chaperone that binds to and prevents the accumulation of misfolded proteins,
577 particularly during the innate immune response. Exposure to HOCl was found to further
578 improve the chaperone function of α_2M, but the mechanism remained unclear [32].

579 To test whether the previously observed effect is due to *N*-chlorination, we treated α_2M with a
580 10- and 50-fold molar excess of HOCl (corresponding to 0.3 mM and 1.5 mM HOCl,
581 respectively), followed by the addition of the antioxidant ascorbate for re-reduction. In line with
582 expectations, chaperone activity of α_2M increased with the amount of HOCl added (Fig. 5 a,
583 b). Treatment with ascorbate, as well as methylation of basic amino acid residues prior to HOCl
584 exposure fully inhibited the chaperone activation of HOCl-modified α_2M. These results
585 strongly support the notion that HOCl-induced *N*-chlorination of basic amino acid side chains
586 also accounts for the increased chaperone activity of α_2M.

587 Intriguingly, we also observed similar chaperone-like conversion upon HOCl treatment for
588 Cohn fraction IV and the γ-globulin fraction (Fig. 5 c-f). In both cases, however, efficient
589 activation of the chaperone activity required higher HOCl concentrations. It is important to
590 note, however, that all HOCl concentrations used were below the range known to be generated
591 directly at sites of inflammation [31]. While exposure of Cohn fraction IV to an estimated 10-fold
592 molar excess of HOCl (corresponding to 2 mM HOCl) had only little effect on citrate synthase

593 aggregation, treatment with a 50-fold molar excess of HOCl strongly activated chaperone-like
594 properties (Fig. 5 c, d). This chaperone activity was markedly reduced, but not completely
595 inhibited, after reduction with ascorbate. Likewise, methylation of amine side chains prior to
596 HOCl exposure did not fully abrogate the chaperone-like conversion of this protein fraction.
597 Similarly, activation of the chaperone function of the γ-globulin fraction occurred at higher
598 HOCl concentrations ranging from 4.3 mM to 13 mM (corresponding to an estimated 50- to
599 150-fold molar excess of HOCl). Strikingly, while chaperone activity increased with the
600 amount of HOCl added, reversibility of the chaperone function by ascorbate decreased (Fig. 5
601 e, f).
602 These results suggest that at least some proteins in both plasma fractions tested are transformed
603 to chaperones upon modification by HOCl. Efficient activation of their chaperone function is
604 strongly, but, unlike HSA, not exclusively linked to *N*-chlorination, suggesting some other
605 HOCl-induced modifications that cannot be removed by ascorbate in these plasma proteins.

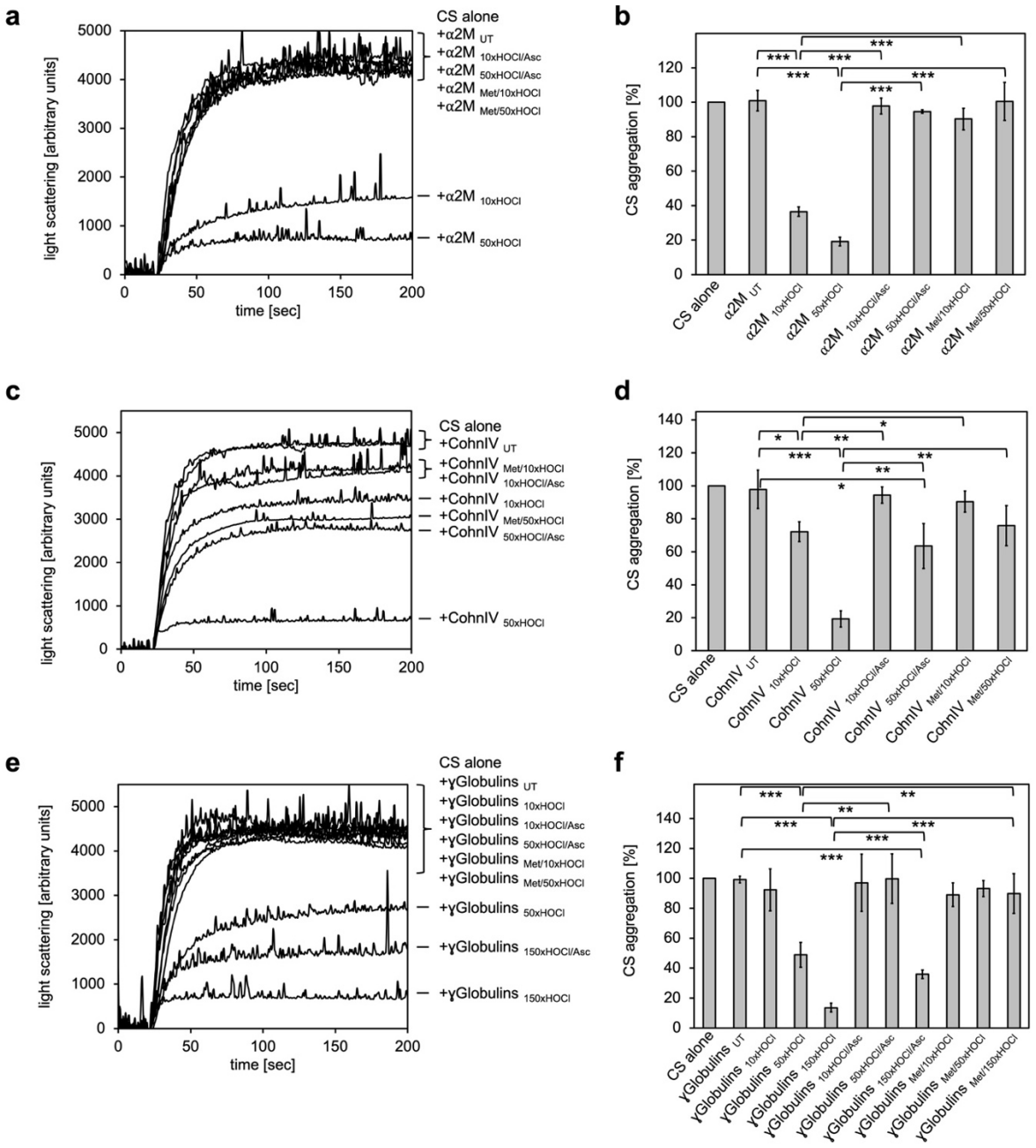

Figure 5: All plasma protein fractions tested exhibit reversible chaperone activity upon modification by HOCl. α_2-Macroglobulin (**a**, **b**), Cohn fraction IV (**c**, **d**) and the γ-globulin fraction (**e**, **f**) were analyzed for chaperone activity in a citrate synthase aggregation assay upon treatment with various doses of HOCl. Each plasma protein fraction, when treated with a 10-, 50- or 150-fold molar excess of HOCl, significantly decreased aggregation of chemically-denatured citrate synthase as measured by light scattering at 360 nm**.** Exposure of the various HOCl-treated plasma proteins to the reductant ascorbate significantly decreased or completely inhibited their chaperone function. Methylation of basic amino acid residues prior to HOCl treatment mostly prevented chaperone-like conversion of the plasma proteins. In **a**, **c** and **e** representative measurements are shown. In **b, d** and **f** data are depicting means and standard deviations from three independent experiments. Student's t-test: *$p < 0.05$, **$p < 0.01$, ***$p < 0.001$. Aggregation of citrate synthase in the absence of any plasma protein fraction was set to 100% and all the data are presented as percentage of this control. Labels of aggregation curves are written in the order of the final intensity of light scattering of the respective treatment.

619 **HOCl-induced *N*-chlorination converts the majority of plasma proteins into activators of**
620 **neutrophil-like cells**

621 Ours and others findings indicate that *N*-chlorinated serum albumin is a key factor for the
622 stimulation of leukocytes at sites of inflammation. To test if also other plasma proteins exert
623 this function upon HOCl exposure, we analyzed the NADPH oxidase-dependent generation of
624 superoxide by differentiated PLB-985 cells in the presence of various treated plasma protein
625 fractions, as described above.

626 Addition of α_2-macroglobulin, treated with a 50-fold molar excess of HOCl (i.e. 1.5 mM
627 HOCl), did not enhance superoxide production (Fig. 6 a, b). In contrast, exposure to the same
628 molar excess of HOCl, corresponding to 10 mM HOCl in this case, converted at least some
629 proteins of Cohn fraction IV into highly efficient stimulators of the neutrophil NADPH oxidase
630 (Fig. 6 c, d). Analysis of the kinetics showed that activation by this HOCl-treated protein
631 fraction occurred at a similar rate as the activation by PMA. Such a stimulatory effect was also
632 observed for the γ-globulin fraction upon treatment with an estimated 150-fold molar excess of
633 HOCl (i.e. 13 mM). The minimum HOCl concentration required for the activating function of
634 these plasma proteins was thus 10 mM and conformed to the range of HOCl concentrations
635 expected under inflammatory conditions. Importantly, the activating effect of both HOCl-
636 treated plasma fractions was completely abolished upon reduction with ascorbate or by prior
637 methylation of their amino groups, strongly suggesting that *N*-chlorination is the responsible
638 mechanism for the functional switch of these proteins into efficient activators of neutrophil-like
639 cells as well.

640 These findings demonstrate that HOCl-mediated *N*-chlorination constitutes a key mechanism
641 to increase the immunogenicity of plasma proteins under inflammatory conditions. Upon
642 modification, not only serum albumin, but the majority of the plasma fractions tested, form a
643 feed-forward inflammatory loop to amplify and sustain inflammatory responses which can lead
644 to accelerated pathogen clearance but could also contribute to chronic inflammation.

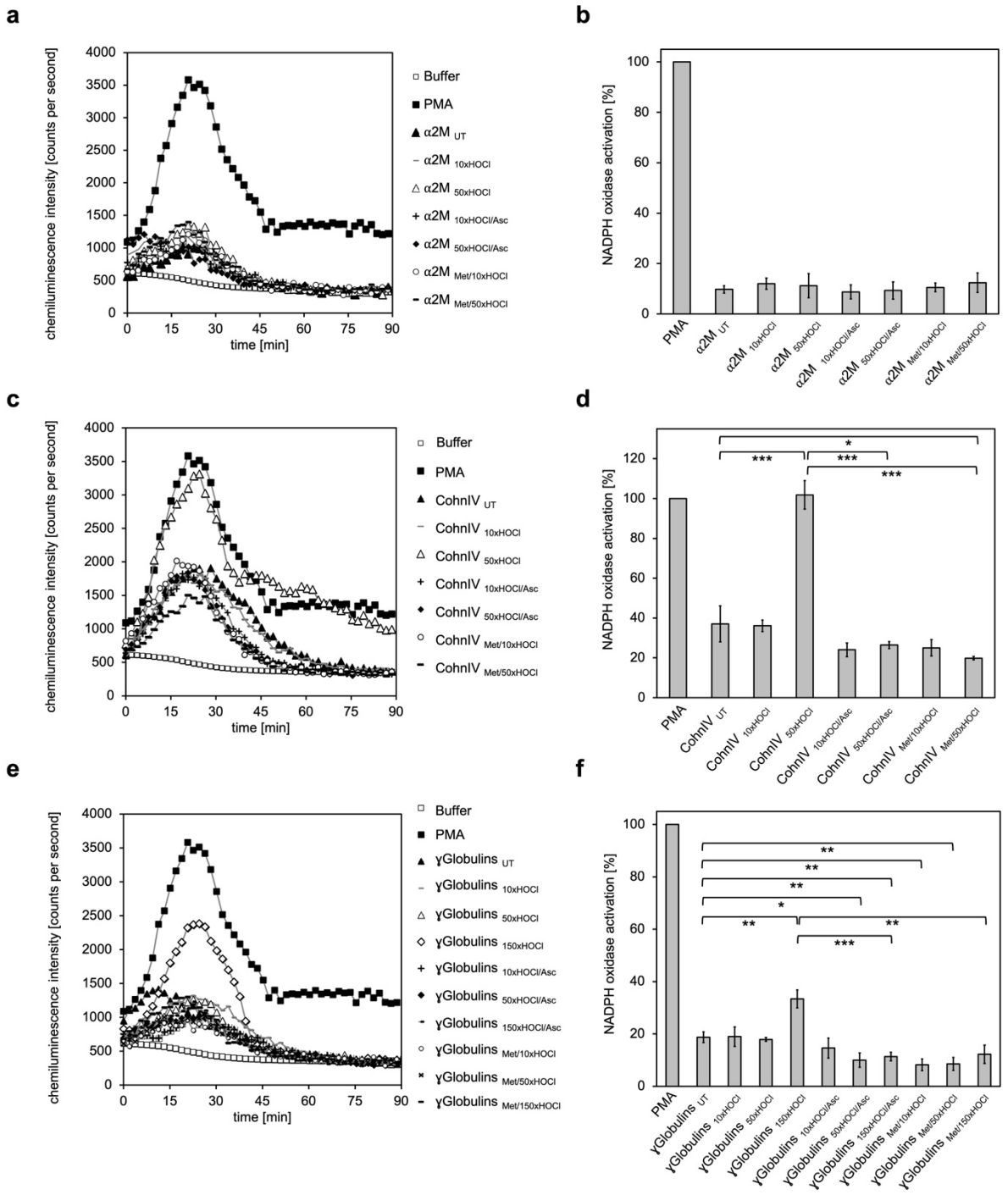

Figure 6: The majority of human plasma proteins stimulate neutrophil respiratory burst upon *N*-chlorination by HOCl. The effect of HOCl-treated α_2-macroglobulin (α_2M) (**a**, **b**), Cohn fraction IV (**c**, **d**) and the γ-globulin fraction (**e**, **f**) on the activity of the neutrophil NADPH oxidase was investigated. α_2M, when treated with various doses of HOCl, had no influence on ROS generation by the NADPH oxidase (**a**, **b**). Treatment with a 50- or 150-fold molar excess of HOCl converted at least some proteins of Cohn fraction IV (CohnIV $_{50xHOCl}$) and the γ-globulin fraction (γGlobulins $_{150xHOCl}$), respectively, into efficient inducers of the neutrophil respiratory burst, reflected by the increased production and release of oxidants that induce lucigenin chemiluminescence (**c-f**). The activating function of CohnIV $_{50xHOCl}$ and γGlobulins $_{150xHOCl}$ could be reversed by treatment with the reductant ascorbate (CohnIV $_{50xHOCl/Asc}$ and γGlobulins $_{150xHOCl/Asc}$) and was abrogated by methylation of basic amine side

655 chains prior to HOCl exposure (CohnIV $_{Met/50xHOCl}$ and γGlobulins $_{Met/150xHOCl}$). **(a**, **c**, **e)** Extracellular oxidant
656 production by neutrophil NADPH oxidase was measured in one- to two-minutes intervals over 90 minutes at 37
657 °C using lucigenin-enhanced chemiluminescence. Phorbol 12-myristate 13-acetate (PMA; final concentration (fc),
658 0.2 µM), untreated and the variously treated plasma fraction samples (fc, 2 mg · mL^{-1} for α_2-macroglobulin and 3
659 mg · mL^{-1} for Cohn fraction IV and the γ-globulin fraction) from the previous citrate synthase aggregation assays
660 (see above) or PBS buffer (basal oxidant production) were added to differentiated PLB-985 cells in PBS buffer
661 containing 400 µM lucigenin immediately prior to chemiluminescence measurement. **(b**, **d**, **f)** Results are
662 expressed as integrated total counts (means and standard deviations of three independent measurements) higher
663 than buffer control. Student's t-test: *$p < 0.05$, **$p < 0.01$, ***$p < 0.001$. PMA- induced activation of NADPH-
664 oxidase was set to 100%.

665 **Activation of NADPH oxidase by *N*-chlorinated serum albumin and immunoglobulin G**
666 **occurs predominantly via PI3K-dependent signaling pathways**

667 Activity of the NADPH oxidase complex of neutrophils is regulated by several signaling
668 pathways downstream of cell surface receptors. Central amongst these are PLC/PKC-
669 (phospholipase C/protein kinase C) and PI3K- (phosphoinositide 3-kinase)-dependent
670 pathways, blockade of which severely lowers NADPH oxidase activation by various stimuli
671 such as chemotactic peptides, opsonized particles or phorbol esters [66–69].

672 To identify the predominant signaling mechanism through which the *N*-chlorinated serum
673 albumin and the major component of the γ-globulin fraction, immunoglobulin G, activate the
674 neutrophil respiratory burst, the effect of various inhibitors on the $HSA_{50xHOCl}$ and
675 $IgG_{150xHOCl}$-induced ROS generation was tested. PMA, a direct activator of conventional PKC
676 isoforms such as PKCα and PKCβ was used as a control for PKC-dependent activation of the
677 NADPH oxidase [64].

678 It is worth noting, that all cell suspensions contained DMSO at a final concentration of 1%. As
679 a consequence, NADPH oxidase activation by PMA, $HSA_{50xHOCl}$ or $IgG_{150xHOCl}$ proceeded at a
680 lower rate compared to the previously described experiments (see Figs. 4 and 6), peaking at 35-
681 50 minutes after the addition of these agents to the cells.

682 Pretreatment of neutrophil-like cells with 10 µM diphenyleneiodonium (DPI), a direct inhibitor
683 of the NADPH oxidase complex, for 30 minutes prior to stimulation with PMA, $HSA_{50xHOCl}$ or

684 $IgG_{150xHOCl}$ fully inhibited ROS generation confirming that the ROS production induced by
685 these stimulatory agents was NADPH-oxidase dependent (Fig. 7). In line with expectations,
686 presence of the PI3K inhibitor wortmannin (100 nM) had only little effect on the PMA-
687 mediated activation of the NADPH oxidase (Fig. 7 c, d). In contrast, wortmannin strongly
688 attenuated the $HSA_{50xHOCl}$- and $IgG_{150xHOCl}$-induced ROS generation by the immune cells,
689 suggesting a PI3K-dependent mechanism of NADPH oxidase activation (Fig. 7 a, b, d). Along
690 this line, pretreatment with 200 nM Gö 6983, that selectively inhibits several PKC isozyme
691 families, including the classical PKCα and PKCβII, the novel PKCδ and the atypical PKCζ,
692 strongly inhibited NADPH oxidase activation by PMA, but not by $HSA_{50xHOCl}$ and $IgG_{150xHOCl}$.
693 These results suggest that PI3K is the key signaling component in the pathway that leads to
694 $HSA_{50xHOCl}$ – and $IgG_{150xHOCl}$- dependent activation of the neutrophil NADPH oxidase.

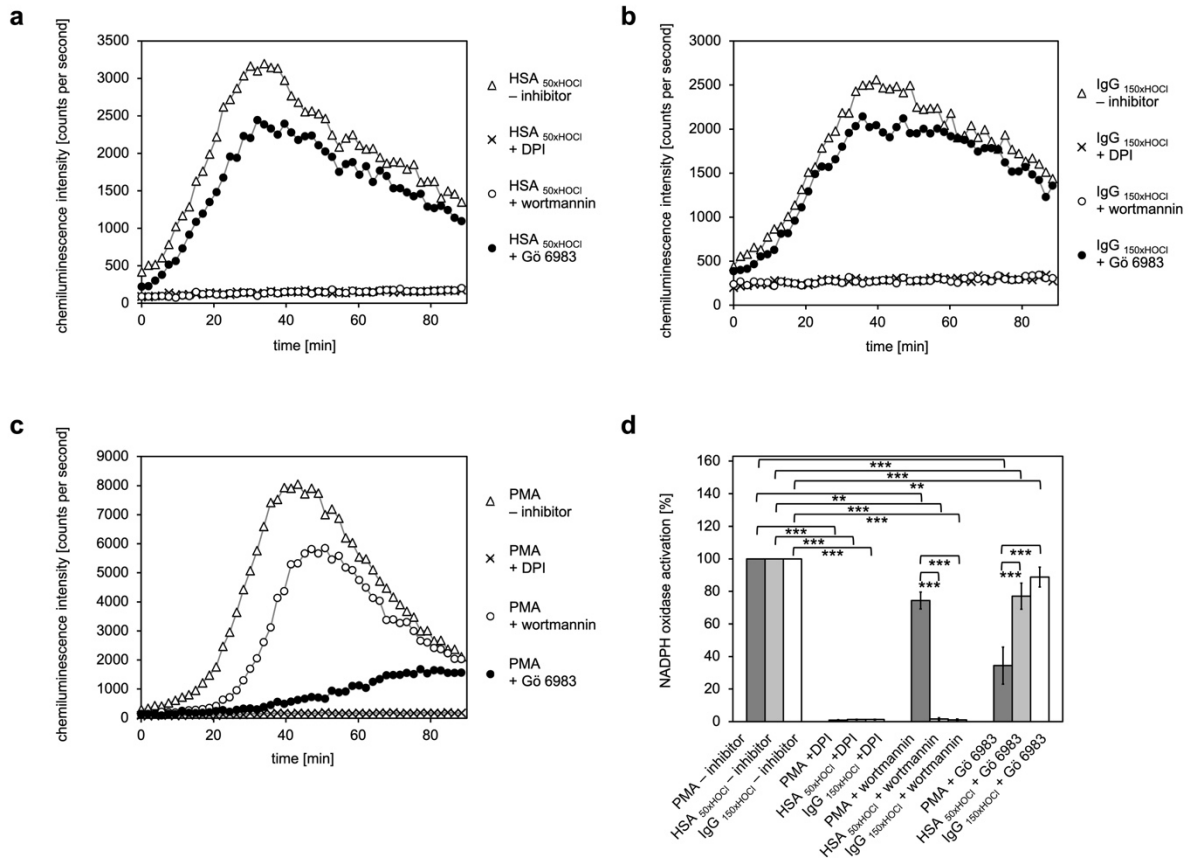

Figure 7: Activation of the NADPH oxidase of neutrophil-like cells by HOCl-treated serum albumin and immunoglobulin G occurs predominantly via a PI3K-dependent signaling pathway. Effect of 10 µM diphenyleneiodonium (DPI; NADPH oxidase inhibitor), 100 nM wortmannin (PI3K inhibitor) and 200 nM Gö 6983 (protein kinase C (PKC) inhibitor) on the NADPH oxidase activation mediated by **(a)** 3 mg · mL^{-1} $HSA_{50xHOCl}$, **(b)** 3 mg · mL^{-1} $IgG_{150xHOCl}$ and **(c)** 0.2 µM PMA was tested. **(d)** Results shown in **a**, **b** and **c** are expressed as integrated total counts (means and standard deviations of three independent measurements) higher than the respective buffer control. Student's t-test: **p < 0.01, ***p < 0.001.

HOCl-treated serum albumin promotes survival of neutrophil-like cells in the presence of the foreign protein antigen Ag85B, but not in the presence of staurosporine

As shown previously, activation of the NADPH oxidase by HOCl-modified serum albumin involves the action of PI3K. Since PI3K is a key component of the well-documented, anti-apoptotic PI3K/Akt signaling pathway [70], it was tempting to speculate that HOCl-modified HSA could promote cell survival in the presence of noxious stimuli. To test this hypothesis, we exposed neutrophil-like PLB-985 cells to the highly immunogenic mycobacterial protein antigen Ag85B and staurosporine in the presence of native or HOCl-treated HSA. The

711 mycolyltransferase Ag85B is the major antigen produced and secreted from all mycobacterial
712 species during infection [71] and has been shown to play an important role in the induction of
713 protective immunity [72,73] by inducing strong T cell proliferation and IFN-γ secretion [74,75].
714 Activation of neutrophils during mycobacterial infections is often accompanied by accelerated
715 apoptosis [76,77], but the mechanism by which mycobacterial species or their secreted antigens
716 induce apoptosis has not been elucidated in detail. Staurosporine, a protein kinase inhibitor, has
717 been characterized as an efficient inducer of apoptosis in various cell types via caspase-
718 dependent and -independent pathways [78,79] and thus, was also used as an cell death-promoting
719 agent in our experiments.
720 After one hour or six hours of incubation with Ag85B and staurosporine, respectively, viability
721 of the variously treated cells was evaluated by flow cytometry using Annexin V-
722 FITC/propidium iodide (PI) staining. During early apoptosis, phosphatidylserine is translocated
723 from the inner to the outer cell membrane leaflet with the plasma membrane left intact and thus,
724 available for binding of extrinsically applied annexin V protein [80]. In late apoptosis/necrosis,
725 the integrity of the plasma membrane is lost, allowing the normally membrane-impermeable
726 propidium iodide to enter and stain the DNA. Cells that are in late apoptosis or necrotic are thus
727 both Annexin V-FITC and PI positive. Accordingly, cells that are viable are both Annexin V-
728 FITC and PI negative.
729 Data plots were generated from analysis of ungated data (Fig. 8). Viable cells appear in the
730 lower left quadrant (Q4), early apoptotic cells in lower right quadrant (Q3) and late
731 apoptotic/necrotic cells in the upper right (Q2) quadrant.
732 Upon treatment with Ag85B, the ratio of viable cells to early/late apoptotic cells has markedly
733 decreased compared to the control cells, that were incubated in the absence of Ag85B, pointing
734 towards a lifetime-limiting effect of Ag85B. Pretreatment with the broad-spectrum pan-caspase
735 inhibitor Z-VAD-FMK did not significantly affect Ag85B-induced cell death, suggesting that
736 Ag85B exerts its lethal effect through a caspase-independent mechanism. To test whether the

737 toxicity of Ag85B depends on its uptake by the immune cells, we pretreated the cells with
738 cytochalasin D, an inhibitor of phagocytosis, prior to the addition of Ag85B. Reduction of the
739 cells' phagocytic capacity resulted in markedly improved cell survival in the presence of
740 Ag85B. This phenomenon is illustrated by a shift of the cells from Q3 to Q4 on the Annexin
741 V-FITC/PI plot with concomitant reduction of necrotic cells. Remarkably, pretreatment with
742 HOCl-modified HSA, added at a 155-fold molar excess over Ag85B, completely prevented cell
743 death upon addition of Ag85B. In contrast, native HSA had almost no effect on Ag85B-induced
744 cell death. We thus speculated that HOCl-treated HSA could rescue immune cells from Ag85B-
745 induced cell death by preventing or strongly reducing its uptake, rather than by boosting
746 PI3K/Akt signaling. In support of this conclusion, Z-VAD-FMK, but not HOCl-treated HSA
747 was able to significantly reduce staurosporine-induced apoptosis. Instead, when combined with
748 staurosporine, HOCl-modified HSA triggered necrosis with the majority of the cells being
749 Annexin V and PI positive.

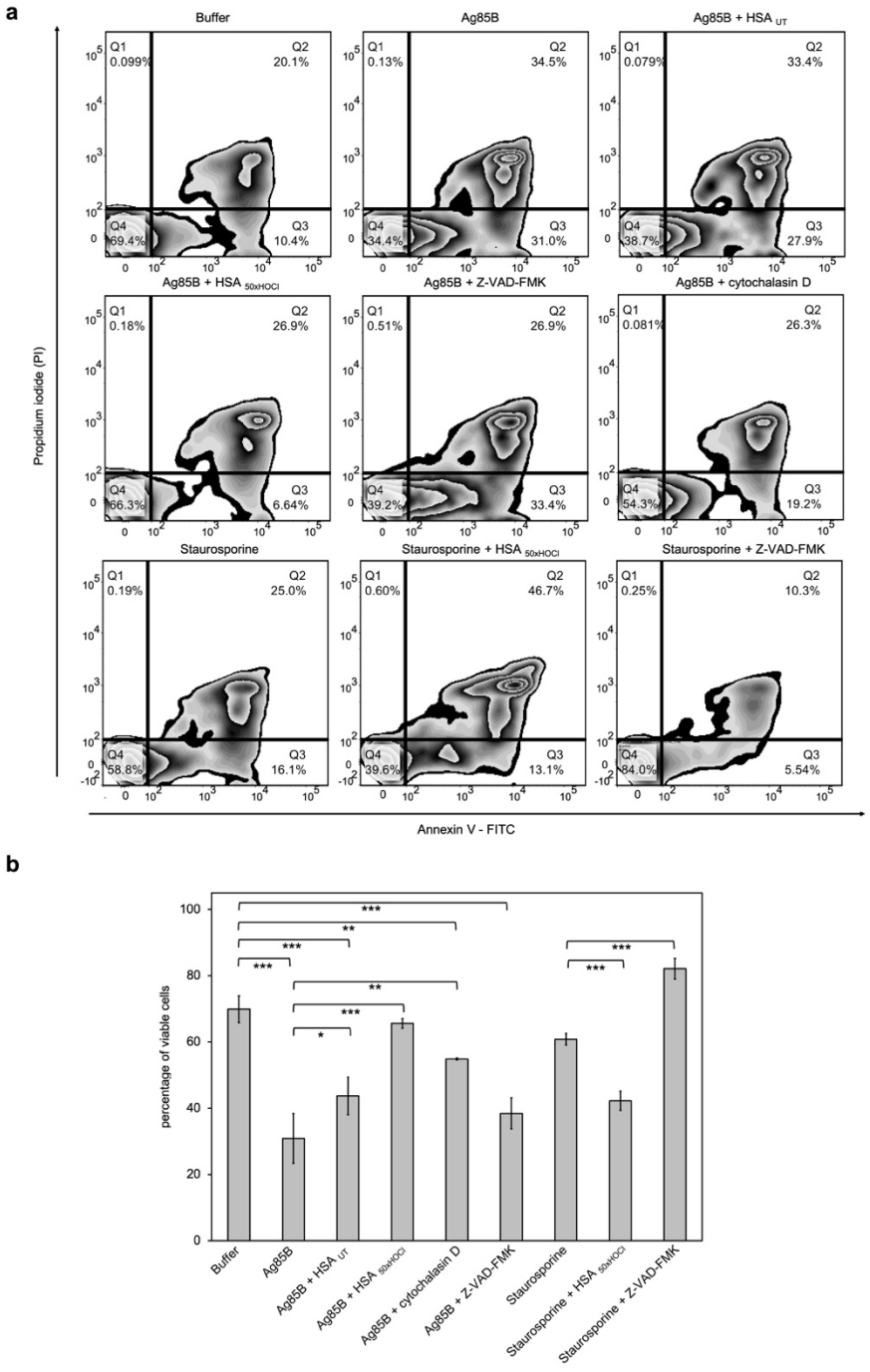

Figure 8: HOCl-treated serum albumin improves survival of neutrophil-like cells in the presence of the major mycobacterial protein antigen Ag85B. Differentiated neutrophil-like PLB-985 cells were preincubated with 50 µM Z-VAD-FMK, 155 µM native (HSA_{UT}) or HOCl-treated HSA ($HSA_{50xHOCl}$) prior to the addition of 1 µM Ag85B or 2 µM staurosporine. After one hour (Ag85B) or six hours (staurosporine) of incubation, viability of the variously treated cells was assessed by flow cytometry using Annexin V/propidium iodide (PI) staining. Cells treated only with buffer served as control. **(a)** Annexin V-FITC vs. propidium iodide dot plots show all analyzed events. Staining of cells simultaneously with Annexin V- FITC (green fluorescence) and the non-vital dye PI (red fluorescence) allows the discrimination of viable, intact cells (FITC-, PI-; Q4), early apoptotic (FITC+, PI-; Q3) and late apoptotic/necrotic cells (FITC+, PI+; Q2). 20,000 events were acquired and recorded per sample. Data were analyzed using FlowJo (version 10) software. Results shown are representative of three experiments.

761 **(b)** Results of three independent experiments for viable cells are shown (means and standard deviations). Student's
762 t-test: *$p < 0.05$, **$p < 0.01$, ***$p < 0.001$.

763 **HOCl-treated serum albumin effectively binds Ag85B and reduces its uptake by**
764 **neutrophil-like cells**

765 Prompted by the finding that HOCl-treated HSA can act as a chaperone being highly effective
766 at preventing protein aggregation, we asked whether *N*-chlorinated HSA can also bind to
767 Ag85B and thus prevent its uptake by immune cells. To test this, Ag85B was diluted stepwise
768 in the presence of native or HOCl-treated HSA and aggregation of Ag85B was monitored by
769 light scattering. When denatured Ag85B was diluted into buffer, it readily formed aggregates
770 (Fig. 9 a, b). This aggregation could not be prevented by untreated HSA. Presence of HOCl-
771 modified HSA, however, significantly reduced the aggregation of Ag85B when added at a 80-
772 fold molar excess over the protein. Again, reduction with ascorbate fully abrogated HSA_{HOCl}'s
773 ability to bind Ag85B.

774 We argued that Ag85B's association with HOCl-modified HSA could decrease its propensity
775 to enter immune cells and thus, provide a possible explanation for the enhanced survival of
776 neutrophils in the presence of this mycobacterial antigen. To test whether this HSA_{HOCl} -
777 mediated cell survival is indeed due to a reduced uptake, we added recombinant fluorescently-
778 labeled Ag85B (Ag85B-488) to differentiated neutrophil-like cells and analyzed its uptake in
779 the presence of native or HOCl-treated HSA using flow cytometry. Cells conincubated with
780 native HSA accumulated around 30% less Ag85B compared to cells treated with Ag85B alone
781 (Fig. 9 c, d). But presence of HOCl-treated HSA reduced uptake of Ag85B by up to 80%.
782 Sustained cell viability in the presence of Ag85B is thus most likely linked to decreased antigen
783 uptake by the immune cells.

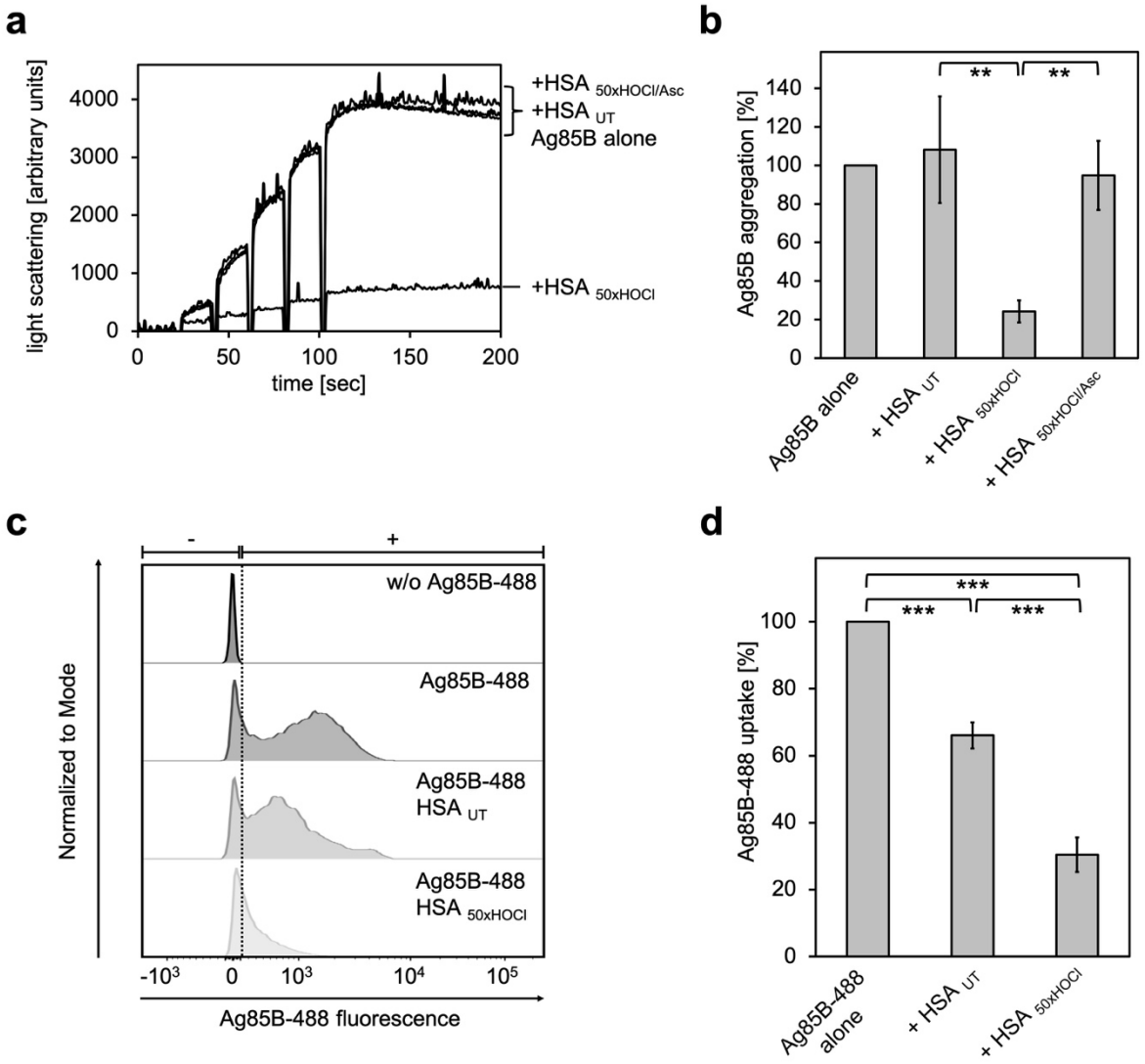

Figure 9: HOCl-treated serum albumin binds to and prevents uptake of the major mycobacterial protein antigen Ag85B by neutrophil-like cells. (a, b) HSA, treated with a 50-fold molar excess of HOCl ($HSA_{50xHOCl}$) significantly decreased aggregation of denatured Ag85B as measured by light scattering at 360 nm. Reduction of $HSA_{50xHOCl}$ with a 50-fold molar excess of the antioxidant ascorbate ($HSA_{50xHOCl/Asc}$) reversed this chaperone activity. **(a)** A representative measurement of Ag85B aggregation in the presence of native HSA (HSA_{UT}), $HSA_{50xHOCl}$ and $HSA_{50xHOCl/Asc}$ is shown. Labels of aggregation curves are written in the order of the final intensity of light scattering of the respective treatment. **(b)** Data are represented as means and standard deviations from three independent aggregation assays. Aggregation of Ag85B in the absence of HSA was set to 100% and all the data are presented as percentage of this control. **(c, d)** Differentiated neutrophil-like PLB-985 cells were incubated in the absence or presence of the fluorescently-labeled Ag85B protein, Ag85B-488. In some cases, HSA_{UT} or $HSA_{50xHOCl}$ was added at a 50-fold molar excess over Ag85B-488 to the cells. After one hour of incubation, uptake of fluorescent Ag85B-488 by the variously treated cells was assessed by flow cytometry. 30,000 events were acquired and recorded per sample. Data were analyzed using FlowJo (version 10) software. **(c)** Single-parameter histogram overlays of Ag85B-488 fluorescence of the various samples are shown. **(d)** Results of three independent experiments are shown (means and standard deviations). Student's t-test: $^{**}p < 0.01$, $^{***}p < 0.001$. Uptake of Ag85B-488, reflected by the median fluorescence intensity, in the absence of HSA was set to 100%.

801 **DISCUSSION**

802 Myeloperoxidase (MPO)-derived HOCl is one of the strongest oxidants produced and released
803 by neutrophils during infection and inflammation (recently reviewed in ref. [42]). Because of its
804 high reactivity with a wide variety of biomolecules, HOCl forms an efficient weapon against a
805 wide range of pathogens, but also contributes to host tissue injury associated with diverse
806 inflammatory diseases [81]. Due to their high abundance in blood and interstitial fluid, plasma
807 proteins constitute major targets for HOCl-mediated modification with thiol oxidation and
808 chlorination of amine side chains being the favored reactions [22], followed by some irreversible
809 modifications including tryptophan oxidation, peptide bond cleavage or di-tyrosine cross-
810 linking [82], when exposed to high doses of HOCl as those present at sites of chronic
811 inflammation. Formation and accumulation of such advanced oxidation protein products
812 (AOPPs) is indeed a hallmark of various inflammatory diseases [44,83].

813 Aside from their role as important scavengers of the majority of generated HOCl [39,84], there is
814 a growing body of evidence demonstrating protective and/or immunomodulatory function of
815 these AOPPs during inflammation. α_2-Macroglobulin (α_2M), a plasma glycoprotein, already
816 acts as an extracellular chaperone capable of suppressing the aggregation of a range of proteins
817 [85], but modification by HOCl has been reported to drastically increase its chaperone activity by
818 a yet unknown mechanism [32]. Previously, we observed a similar phenomenon in *E. coli*, where
819 the protein RidA, a member of the YjgF/YER057c/UK114 protein family, was converted into
820 an efficient chaperone holdase upon exposure to HOCl by a mechanism that involved the
821 reversible chlorination of its basic amino acids [17]. This finding was rather surprising, since
822 activation of other known redox-regulated chaperones, such as Hsp33 or 2-cys peroxiredoxins
823 [19,86], by HOCl occured via oxidation of their cysteine residues and not by *N*-chlorination, a
824 modification that before our study has been thought to have a mostly deleterious effect on
825 protein function. Since similar observations were made more recently for *E. coli* CnoX (YbbN)
826 [25] and the HSA homologue bovine serum albumin (BSA) [17], HOCl-mediated *N*-chlorination

827 can, therefore, be considered a novel, cysteine-independent and reversible mechanism of
828 chaperone activation in response to HOCl-stress.
829 Encouraged by these findings, we hypothesized that HOCl-mediated improvement of α_2M's
830 chaperone function may be also based on *N*-chlorination and suspected that α_2M could be not
831 the only plasma protein exhibiting chaperone activity upon modification by HOCl. In fact, we
832 found that not only α_2M but a number of proteins in all plasma fractions tested turned into
833 chaperone-like proteins, being highly effective at preventing formation of potentially toxic
834 protein aggregates *in vitro*. The role of plasma proteins in inflamed tissue thus goes beyond that
835 of a passive sink for HOCl.
836 Since exposure to high HOCl concentrations can lead to oxidative, irreversible protein
837 unfolding [16], one might speculate that the observed chaperone activity of such unfolded plasma
838 proteins could simply be the result of an increased affinity to other unfolded proteins. Here, we
839 provide direct evidence that HOCl-mediated conversion of plasma proteins into potent
840 chaperones depends primarily on reversible chlorination of their basic amino acids. Along this
841 line, treatment of HSA with HOCl led to dose-dependent reduction of the accessible amino
842 group content accompanied by an increase in surface hydrophobicity, providing an obvious
843 explanation for the increased affinity to unfolding proteins of *N*-chlorinated plasma proteins.
844 Since *N*-chlorination does not irreversibly alter the structural and functional properties of a
845 protein, this reversible post-translational modification provides a new strategy to recruit new
846 chaperone-like proteins on demand in response to HOCl-stress in order to minimize self-
847 damage associated with the formation of protein aggregates during inflammation.
848 In recent years, other roles for HOCl-modified plasma proteins and lipoproteins in
849 inflammatory processes have also been described. For example, HOCl-oxidized low-density
850 lipoproteins [87] as well as HOCl-modified HSA [47,48] have been shown to elicit various
851 polymorphonuclear leukocyte (PMNL) responses such as the NADPH-dependent generation of
852 reactive oxygen species (ROS), degranulation or shape change [47], but the mechanism for the

853 HOCl-mediated functional conversion into a potent activator of human PMNLs remained
854 unclear.
855 As *N*-chlorination was the principal chemical modification responsible for the plasma protein's
856 switch to a chaperone-like holdase, we hypothesized that it could also be the reason for the
857 activation of immune cells. To mimic an *in vivo* situation, where plasma proteins are located in
858 immediate vicinity to accumulated neutrophils in inflamed tissue, we exposed several plasma
859 fractions to HOCl at pathophysiological concentrations [31] and investigated the effect of the
860 resulting products on ROS production by neutrophil-like cells. Remarkably, we found that not
861 only the main plasma protein HSA, but the majority of plasma fractions tested, when treated
862 with a sufficient amount of HOCl, were able to elicit a significant immune response, as shown
863 by the increased generation of ROS by the immune cells. This effect was not seen upon re-
864 reduction of the HOCl-modified proteins or prior methylation of their basic amino acids,
865 strongly supporting a *N*-chlorination based mechanism as well. To the best of our knowledge,
866 this is the first study which demonstrates that reversible HOCl-mediated *N*-chlorination is the
867 principal mechanism of turning plasma proteins into critical modulators of the innate immune
868 response.
869 Gorudko et al. reported that the phosphoinositide 3-kinase (PI3K) inhibitor wortmannin
870 inhibited the stimulating effect of HOCl-modified HSA on immune cells [47]. The same was true
871 in our model system: the immunomodulatory action of both HOCl-modified HSA and
872 immunoglobulin G could be fully inhibited or strongly attenuated by wortmannin. PI3K and its
873 downstream effectors, such as the serine/threonine kinase Akt, are indeed considered to play a
874 key role in the regulation of the neutrophil NADPH oxidase [88,89]. Since the PKC inhibitor Gö
875 6983 showed only little effect on $HSA_{50xHOCl}$- and $IgG_{150xHOCl}$-mediated NADPH oxidase
876 activation, we thus propose that these proteins stimulate the neutrophil respiratory burst
877 predominantly via PI3K-dependent signaling pathways. However, further studies are needed to
878 investigate the exact mechanism by which these proteins trigger PI3K signaling. A possible

879 scenario might be, that *N*-chlorination confers higher affinity to a membrane scavenger receptor
880 allowing the binding of HOCl-modified HSA. In support of this theory, it has been reported
881 that *N*-chlorinated, but not native HSA can irreversibly bind to and block the major high-density
882 lipoprotein receptor, scavenger receptor class B, type 1 (SR-BI) [90]. It is therefore tempting to
883 speculate that *N*-chlorination could also increase the affinity of IgG to Fc gamma receptors
884 (FcγRs).

885 The PI3K/Akt pathway is also considered an anti-apoptotic pathway [91,92]. Thus, it was tempting
886 to hypothesize that HOCl-modified HSA may play a role as a pro-survival molecule during
887 inflammation. Remarkably, we found that HOCl-modified HSA indeed enhances survival of
888 neutrophils in the presence of the highly immunogenic mycobacterial protein antigen Ag85B,
889 however, not in the presence of staurosporine, a broad spectrum protein kinase inhibitor that
890 induces apoptosis in various cell types [78,79]. Looking for a mechanism by which HOCl-modified
891 HSA is able to rescue immune cells from Ag85B-induced cell death, we found that it can
892 effectively bind to and strongly decrease the phagocytosis of Ag85B. Internalization of Ag85B
893 by the cells proved to be the direct cause of cell death and could also be prevented by other
894 inhibitors of phagocytosis.

895 Neutrophils are typically short-lived, but their apoptosis can be delayed both by microbial
896 products and by various proinflammatory stimuli [93,94]. In this study, we describe HOCl-
897 modified HSA as a novel pro-inflammatory mediator, which can promote cell survival by
898 binding to highly immunogenic foreign antigens and reducing their phagocytosis at sites of
899 bacterial infection. A similar phenomenon was observed in other studies, where HOCl-
900 modified HSA was shown to bind and neutralize proteins from HIV and West Nile virus [95,96].

901 The immunomodulatory effects of *N*-chlorinated plasma proteins found in this and previous
902 studies constitute a double-edged sword. Although stimulation of neutrophil respiratory burst
903 and enhanced neutrophil survival may be beneficial for pathogen elimination at the initial stage
904 of infection, it can eventually perpetuate a positive feedback loop and contribute to the

905 development and progression of chronic inflammation (Fig. 10). Secretion of HOCl and other
906 oxidants by permanently activated neutrophils leads not only to the destruction of neighboring,
907 healthy cells resulting in tissue injury [26,97,98], but generates more *N*-chlorinated plasma proteins.
908 Similarly, the pro-survival effect of *N*-chlorinated HSA is not only positive, as cell death and
909 the subsequent recognition of dying neutrophils by macrophages has a critical function in the
910 resolution of the inflammatory response and is strictly required to protect the surrounding tissue
911 and prevent pathological sequelae [99]. Were all these properties of AOPPs dependent on the
912 numerous irreversible modifications reportedly caused by HOCl exposure, this could lead to a
913 spreading out-of-control immune reaction. The presence of high concentrations of antioxidants
914 such as ascorbate and glutathione in plasma, both of which can reduce *N*-chlorination, provide
915 a mechanism to contain the immune reaction at the site of inflammation. Indeed, depletion of
916 these antioxidants is often associated with chronic inflammation and other diseases [100–103] and
917 antioxidant therapy such as high-dose intravenous vitamin C treatment leads to decrease of
918 inflammation markers such as CRP [104–106]. Our data explains important aspects of these effects
919 and further highlights the role of antioxidant homeostasis in inflammatory processes.
920 In summary, our data support a critical role for HOCl-mediated *N*-chlorination of plasma
921 proteins during inflammatory processes and suggest that it is the critical modification mediating
922 the physiological effects of so-called AOPPs. Although the reversible conversion of HOCl-
923 modified plasma proteins to effective chaperones confers protection against HOCl-induced
924 protein aggregation, the increase of their immunogenicity can potentially exacerbate self-
925 damage at sites of inflammation through a positive feedback loop. The fact that the activation
926 of immune cells is mediated through *N*-chlorination, a modification that is reversible by
927 antioxidants present in plasma, provides a mechanism to attenuate or deactivate this positive
928 feedback loop. These findings contribute importantly to our understanding of the development
929 and progression of chronic inflammation.

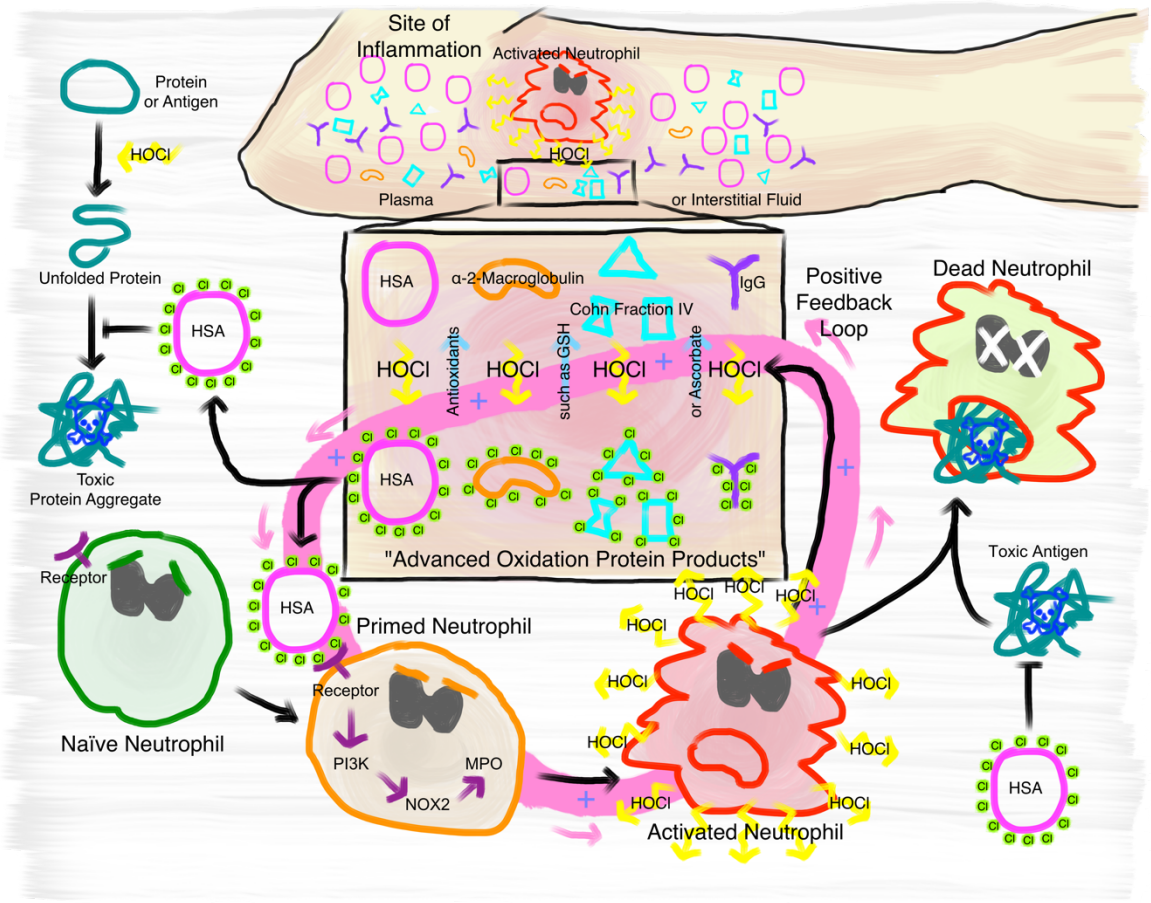

Figure 10: Proposed mechanism of the immunomodulatory role of *N*-chlorination of plasma proteins at a site of inflammation. At the site of inflammation neutrophils (and potentially other immune cells) are activated. Neutrophils then produce HOCl at concentrations of up to 25 to 50 mM per hour. Plasma proteins, such as HSA, α- and β-globulins (Cohn Fraction IV), γ-globulins (IgG), and α_2-Macroglobulin then act as an effective sink. Reversible *N*-chlorination of these proteins turns them into effective chaperons, which can prevent the formation of protein aggregates and their uptake by immune cells, enhancing the survival of neutrophils in the presence of toxic antigens. *N*-chlorinated plasma proteins also activate more immune cells, which then in turn produce more HOCl, leading to the formation of more *N*-chlorinated plasma proteins. This positive feedback loop can be attenuated and deactivated by antioxidants present in plasma, such as ascorbate and reduced glutathione (GSH).

941 **ACKNOWLEDGMENTS**

942 Funding for this study was provided by the German Research Foundation (DFG) through grant
943 LE2905/1-2 to LIL as part of the priority program 1710 'Dynamics of Thiol-based Redox
944 Switches in Cellular Physiology'. Parts of this manuscript were written during a Writing Retreat
945 funded by the Ruhr-Universität Bochum Research School RURS^{plus}.

946 **CONFLICT OF INTEREST STATEMENT**

947 The authors have no conflicting financial interests.

948 **AUTHOR CONTRIBUTIONS**

949 AU, AVS, AM, and LIL conceptualized the study. AU, AVS and AM performed the
950 experiments. AU and AVS analyzed the results. NL purified α_2-Macroglobulin and Ag85B.
951 AVS consulted on the manuscript and AU and LIL wrote the manuscript.

952 **REFERENCES**

953

954 1. Mortaz, E., Alipoor, S. D., Adcock, I. M., Mumby, S. & Koenderman, L. Update on
955 Neutrophil Function in Severe Inflammation. *Front. Immunol.* **9**, 2171 (2018).
956 2. Thomas, D. C. The phagocyte respiratory burst: Historical perspectives and recent
957 advances. *Immunol. Lett.* **192**, 88–96 (2017).
958 3. Furtmüller, P. G., Burner, U. & Obinger, C. Reaction of myeloperoxidase compound I
959 with chloride, bromide, iodide, and thiocyanate. *Biochemistry* **37**, 17923–17930
960 (1998).
961 4. van Dalen, C. J., Whitehouse, M. W., Winterbourn, C. C. & Kettle, A. J. Thiocyanate
962 and chloride as competing substrates for myeloperoxidase. *Biochem. J.* **327 (Pt 2**,
963 487–492 (1997).
964 5. Chapman, A. L. P., Hampton, M. B., Senthilmohan, R., Winterbourn, C. C. & Kettle,
965 A. J. Chlorination of bacterial and neutrophil proteins during phagocytosis and killing
966 of Staphylococcus aureus. *J. Biol. Chem.* **277**, 9757–9762 (2002).
967 6. Rosen, H., Crowley, J. R. & Heinecke, J. W. Human neutrophils use the
968 myeloperoxidase-hydrogen peroxide-chloride system to chlorinate but not nitrate
969 bacterial proteins during phagocytosis. *J. Biol. Chem.* **277**, 30463–30468 (2002).
970 7. Degrossoli, A. *et al.* Neutrophil-generated HOCl leads to non-specific thiol oxidation
971 in phagocytized bacteria. *Elife* **7**, 6290 (2018).
972 8. Clark, R. A., Szot, S., Williams, M. A. & Kagan, H. M. Oxidation of lysine side-chains
973 of elastin by the myeloperoxidase system and by stimulated human neutrophils.
974 *Biochem. Biophys. Res. Commun.* **135**, 451–457 (1986).
975 9. Beck-Speier, I., Leuschel, L., Luippold, G. & Maier, K. L. Proteins released from
976 stimulated neutrophils contain very high levels of oxidized methionine. *FEBS Lett.*
977 **227**, 1–4 (1988).

978 10. Heinecke, J. W. Mass spectrometric quantification of amino acid oxidation products in
979 proteins: insights into pathways that promote LDL oxidation in the human artery wall.
980 *FASEB J.* **13**, 1113–1120 (1999).
981 11. Domigan, N. M., Charlton, T. S., Duncan, M. W., Winterbourn, C. C. & Kettle, A. J.
982 Chlorination of tyrosyl residues in peptides by myeloperoxidase and human
983 neutrophils. *J. Biol. Chem.* **270**, 16542–16548 (1995).
984 12. Sivey, J. D. *et al.* Role of lysine during protein modification by HOCl and HOBr:
985 Halogen-transfer agent or sacrificial antioxidant? *Biochemistry* **52**, 1260–1271 (2013).
986 13. Vissers, M. C. & Winterbourn, C. C. Oxidative damage to fibronectin. I. The effects of
987 the neutrophil myeloperoxidase system and HOCl. *Arch. Biochem. Biophys.* **285**, 53–
988 59 (1991).
989 14. Hawkins, C. L. & Davies, M. J. Hypochlorite-induced damage to proteins: formation
990 of nitrogen-centred radicals from lysine residues and their role in protein
991 fragmentation. *Biochem. J.* **332**, 617–625 (1998).
992 15. Hazell, L. J., van den Berg, J. J. & Stocker, R. Oxidation of low-density lipoprotein by
993 hypochlorite causes aggregation that is mediated by modification of lysine residues
994 rather than lipid oxidation. *Biochem. J.* **302**, 297–304 (1994).
995 16. Heinecke, J. W., Li, W., Daehnke, H. L. & Goldstein, J. A. Dityrosine, a specific
996 marker of oxidation, is synthesized by the myeloperoxidase-hydrogen peroxide system
997 of human neutrophils and macrophages. *J. Biol. Chem.* **268**, 4069–4077 (1993).
998 17. Müller, A. *et al.* Activation of RidA chaperone function by N-chlorination. *Nat.*
999 *Commun.* **5**, 5804 (2014).
1000 18. Chapman, A. L. P., Winterbourn, C. C., Brennan, S. O., Jordan, T. W. & Kettle, A. J.
1001 Characterization of non-covalent oligomers of proteins treated with hypochlorous acid.
1002 *Biochem. J.* **375**, 33–40 (2003).
1003 19. Winter, J., Ilbert, M., Graf, P. C. F., Ozcelik, D. & Jakob, U. Bleach activates a redox-

1004 regulated chaperone by oxidative protein unfolding. *Cell* **135**, 691–701 (2008).
1005 20. Storkey, C., Davies, M. J. & Pattison, D. I. Reevaluation of the rate constants for the
1006 reaction of hypochlorous acid (HOCl) with cysteine, methionine, and peptide
1007 derivatives using a new competition kinetic approach. *Free Radic. Biol. & Med.*
1008 **73**, 60–66 (2014).
1009 21. Arnhold, J., Hammerschmidt, S. & Arnold, K. Role of functional groups of human
1010 plasma and luminol in scavenging of NaOCl and neutrophil-derived hypochlorous acid.
1011 *Biochim. Biophys. Acta* **1097**, 145–151 (1991).
1012 22. Pattison, D. I. & Davies, M. J. Absolute rate constants for the reaction of hypochlorous
1013 acid with protein side chains and peptide bonds. *Chem. Res. Toxicol.* **14**, 1453–1464
1014 (2001).
1015 23. Chesney, J. A., Eaton, J. W. & Mahoney, J. R. Bacterial glutathione: a sacrificial
1016 defense against chlorine compounds. *J. Bacteriol.* **178**, 2131–5 (1996).
1017 24. Peskin, A. V & Winterbourn, C. C. Kinetics of the reactions of hypochlorous acid and
1018 amino acid chloramines with thiols, methionine, and ascorbate. *Free Radic. Biol.*
1019 *& Med.* **30**, 572–579 (2001).
1020 25. Goemans, C. V, Vertommen, D., Agrebi, R. & Collet, J.-F. CnoX Is a Chaperedoxin: A
1021 Holdase that Protects Its Substrates from Irreversible Oxidation. *Mol. Cell* **70**, 614–
1022 627.e7 (2018).
1023 26. Pechous, R. D. With Friends Like These: The Complex Role of Neutrophils in the
1024 Progression of Severe Pneumonia. *Front. Cell. Infect. Microbiol.* **7**, 160 (2017).
1025 27. Thieblemont, N., Wright, H. L., Edwards, S. W. & Witko-Sarsat, V. Human
1026 neutrophils in auto-immunity. *Semin. Immunol.* **28**, 159–173 (2016).
1027 28. Klebanoff, S. J. Myeloperoxidase: friend and foe. *J. Leukoc. Biol.* **77**, 598–625 (2005).
1028 29. Davies, M. J. Myeloperoxidase-derived oxidation: mechanisms of biological damage
1029 and its prevention. *J. Clin. Biochem. Nutr.* **48**, 8–19 (2011).

1030 30. Parker, H., Albrett, A. M., Kettle, A. J. & Winterbourn, C. C. Myeloperoxidase
1031 associated with neutrophil extracellular traps is active and mediates bacterial killing in
1032 the presence of hydrogen peroxide. *J. Leukoc. Biol.* **91**, 369–376 (2012).
1033 31. Summers, F. A., Morgan, P. E., Davies, M. J. & Hawkins, C. L. Identification of
1034 plasma proteins that are susceptible to thiol oxidation by hypochlorous acid and N-
1035 chloramines. *Chem. Res. Toxicol.* **21**, 1832–1840 (2008).
1036 32. Wyatt, A. R. *et al.* Hypochlorite-induced structural modifications enhance the
1037 chaperone activity of human α2-macroglobulin. *Proc Natl Acad Sci USA* **111**, E2081-
1038 90 (2014).
1039 33. Prütz, W. A. Hypochlorous acid interactions with thiols, nucleotides, DNA, and other
1040 biological substrates. *Arch. Biochem. Biophys.* **332**, 110–120 (1996).
1041 34. Carr, A. C., van den Berg, J. J. & Winterbourn, C. C. Chlorination of cholesterol in cell
1042 membranes by hypochlorous acid. *Arch. Biochem. Biophys.* **332**, 63–69 (1996).
1043 35. Winterbourn, C. C., van den Berg, J. J., Roitman, E. & Kuypers, F. A. Chlorohydrin
1044 formation from unsaturated fatty acids reacted with hypochlorous acid. *Arch. Biochem.*
1045 *Biophys.* **296**, 547–555 (1992).
1046 36. Shao, B. *et al.* Myeloperoxidase impairs ABCA1-dependent cholesterol efflux through
1047 methionine oxidation and site-specific tyrosine chlorination of apolipoprotein A-I. *J.*
1048 *Biol. Chem.* **281**, 9001–9004 (2006).
1049 37. Peng, D.-Q. *et al.* Tyrosine modification is not required for myeloperoxidase-induced
1050 loss of apolipoprotein A-I functional activities. *J. Biol. Chem.* **280**, 33775–33784
1051 (2005).
1052 38. Colombo, G. *et al.* Thiol oxidation and di-tyrosine formation in human plasma proteins
1053 induced by inflammatory concentrations of hypochlorous acid. *J. Proteomics* **152**, 22–
1054 32 (2017).
1055 39. Himmelfarb, J. & McMonagle, E. Albumin is the major plasma protein target of

1056 oxidant stress in uremia. *Kidney Int.* **60**, 358–363 (2001).

1057 40. Fogh-Andersen, N., Altura, B. M., Altura, B. T. & Siggaard-Andersen, O. Composition
1058 of interstitial fluid. *Clin. Chem.* **41**, 1522–5 (1995).

1059 41. Witko-Sarsat, V. *et al.* Advanced oxidation protein products as a novel marker of
1060 oxidative stress in uremia. *Kidney Int.* **49**, 1304–1313 (1996).

1061 42. Aratani, Y. Myeloperoxidase: Its role for host defense, inflammation, and neutrophil
1062 function. *Arch. Biochem. Biophys.* **640**, 47–52 (2018).

1063 43. Colombo, G. *et al.* A central role for intermolecular dityrosine cross-linking of
1064 fibrinogen in high molecular weight advanced oxidation protein product (AOPP)
1065 formation. *Biochim. Biophys. Acta* **1850**, 1–12 (2015).

1066 44. Liu, S. X. *et al.* Advanced oxidation protein products accelerate atherosclerosis through
1067 promoting oxidative stress and inflammation. *Arterioscler. Thromb. Vasc. Biol.* **26**,
1068 1156–1162 (2006).

1069 45. Descamps-Latscha, B. *et al.* Advanced oxidation protein products as risk factors for
1070 atherosclerotic cardiovascular events in nondiabetic predialysis patients. *Am. J. Kidney*
1071 *Dis.* **45**, 39–47 (2005).

1072 46. Witko-Sarsat, V. *et al.* AOPP-induced activation of human neutrophil and monocyte
1073 oxidative metabolism: a potential target for N-acetylcysteine treatment in dialysis
1074 patients. *Kidney Int.* **64**, 82–91 (2003).

1075 47. Gorudko, I. V *et al.* Hypohalous acid-modified human serum albumin induces
1076 neutrophil NADPH oxidase activation, degranulation, and shape change. *Free Radic.*
1077 *Biol. & Med.* **68**, 326–334 (2014).

1078 48. Witko-Sarsat, V. *et al.* Advanced oxidation protein products as novel mediators of
1079 inflammation and monocyte activation in chronic renal failure. *J. Immunol.* **161**, 2524–
1080 2532 (1998).

1081 49. Imber, M. J. & Pizzo, S. V. Clearance and binding of two electrophoretic

1082 "fast" forms of human alpha 2-macroglobulin. *J. Biol. Chem.* **256**, 8134–
1083 8139 (1981).
1084 50. Leggio, C., Galantini, L. & Pavel, N. V. About the albumin structure in solution: cigar
1085 Expanded form versus heart Normal shape. *Phys. Chem. Chem. Phys.* **10**, 6741–6750
1086 (2008).
1087 51. Johnstone, A. P. & Thorpe, R. *Immunochemistry in Practice*. (Wiley-Blackwell, 1996).
1088 52. Murphy, K. & Weaver, C. *Janeway's Immunobiology, 9th edition*. (Garland
1089 Science, 2016).
1090 53. Wilkins, M. R. *et al.* Protein identification and analysis tools in the ExPASy server.
1091 *Methods Mol. Biol.* **112**, 531–552 (1999).
1092 54. Udenfriend, S. *et al.* Fluorescamine: a reagent for assay of amino acids, peptides,
1093 proteins, and primary amines in the picomole range. *Science* **178**, 871–872 (1972).
1094 55. Pivot-Pajot, C., Chouinard, F. C., El Azreq, M. A., Harbour, D. & Bourgoin, S. G.
1095 Characterisation of degranulation and phagocytic capacity of a human neutrophilic
1096 cellular model, PLB-985 cells. *Immunobiology* **215**, 38–52 (2010).
1097 56. Tlili, A., Dupré-Crochet, S., Erard, M. & Nüsse, O. Kinetic analysis of phagosomal
1098 production of reactive oxygen species. *Free Radic. Biol. & Med.* **50**, 438–447
1099 (2011).
1100 57. Minkenberg, I. & Ferber, E. Lucigenin-dependent chemiluminescence as a new assay
1101 for NAD(P)H-oxidase activity in particulate fractions of human polymorphonuclear
1102 leukocytes. *J. Immunol. Methods* **71**, 61–67 (1984).
1103 58. De Wit, L., Palou, M. & Content, J. Nucleotide sequence of the 85B-protein gene of
1104 Mycobacterium bovis BCG and Mycobacterium tuberculosis. *DNA Seq.* **4**, 267–70
1105 (1994).
1106 59. Lajiness, D. H. *Trehalose Monomycolate Biosynthesis and Utilization in*
1107 *Mycobacterium tuberculosis*. (University of Toledo, 2011).

1108 60. Temple, A., Yen, T.-Y. & Gronert, S. Identification of specific protein carbonylation
1109 sites in model oxidations of human serum albumin. *J. Am. Soc. Mass Spectrom.* **17**,
1110 1172–80 (2006).
1111 61. Sackett, D. L. & Wolff, J. Nile red as a polarity-sensitive fluorescent probe of
1112 hydrophobic protein surfaces. *Anal. Biochem.* **167**, 228–34 (1987).
1113 62. Aasen, T. B., Bolann, B., Glette, J., Ulvik, R. J. & Schreiner, A. Lucigenin-dependent
1114 chemiluminescence in mononuclear phagocytes. Role of superoxide anion. *Scand. J.*
1115 *Clin. Lab. Invest.* **47**, 673–9 (1987).
1116 63. Ellison, M. A., Thurman, G., Gearheart, C. M., Seewald, R. H., Porter, C. C., &
1117 Ambruso, D. R. INF-γ enhances Nox2 activity by upregulating phox proteins when
1118 applied to differentiating PLB-985 cells but does not induce Nox2 activity by itself.
1119 *PLoS One* **10**, (2015).
1120 64. Wolfson, M., McPhail, L. C., Nasrallah, V. N. & Snyderman, R. Phorbol myristate
1121 acetate mediates redistribution of protein kinase C in human neutrophils: potential role
1122 in the activation of the respiratory burst enzyme. *J. Immunol.* **135**, 2057–62 (1985).
1123 65. Chen, X., Zhong, Z., Xu, Z., Chen, L. & Wang, Y. 2′,7′-Dichlorodihydrofluorescein as
1124 a fluorescent probe for reactive oxygen species measurement: Forty years of
1125 application and controversy. *Free Radic. Res.* **44**, 587–604 (2010).
1126 66. Combadière, C., el Benna, J., Pedruzzi, E., Hakim, J. & Périanin, A. Stimulation of the
1127 human neutrophil respiratory burst by formyl peptides is primed by a protein kinase
1128 inhibitor, staurosporine. *Blood* **82**, 2890–8 (1993).
1129 67. Bissonnette, S. A. *et al.* Phosphatidylinositol 3-phosphate-dependent and -independent
1130 functions of p40phox in activation of the neutrophil NADPH oxidase. *J. Biol. Chem.*
1131 **283**, 2108–19 (2008).
1132 68. Simonsen, A. & Stenmark, H. PX domains: attracted by phosphoinositides. *Nat. Cell*
1133 *Biol.* **3**, E179-82 (2001).

1134 69. Perisic, O. *et al.* The role of phosphoinositides and phosphorylation in regulation of
1135 NADPH oxidase. *Adv. Enzyme Regul.* **44**, 279–98 (2004).
1136 70. Martelli, A. M. *et al.* Nuclear phosphatidylinositol 3,4,5-trisphosphate,
1137 phosphatidylinositol 3-kinase, Akt, and PTen: emerging key regulators of anti-
1138 apoptotic signaling and carcinogenesis. *Eur. J. Histochem.* **51 Suppl 1**, 125–31 (2007).
1139 71. Belisle, J. T. *et al.* Role of the major antigen of Mycobacterium tuberculosis in cell
1140 wall biogenesis. *Science* **276**, 1420–2 (1997).
1141 72. Andersen, P. Effective vaccination of mice against Mycobacterium tuberculosis
1142 infection with a soluble mixture of secreted mycobacterial proteins. *Infect. Immun.* **62**,
1143 2536–44 (1994).
1144 73. Baldwin, S. L. *et al.* Evaluation of new vaccines in the mouse and guinea pig model of
1145 tuberculosis. *Infect. Immun.* **66**, 2951–9 (1998).
1146 74. Launois, P. *et al.* T-cell-epitope mapping of the major secreted mycobacterial antigen
1147 Ag85A in tuberculosis and leprosy. *Infect. Immun.* **62**, 3679–87 (1994).
1148 75. Takamura, S., Matsuo, K., Takebe, Y. & Yasutomi, Y. Ag85B of mycobacteria elicits
1149 effective CTL responses through activation of robust Th1 immunity as a novel
1150 adjuvant in DNA vaccine. *J. Immunol.* **175**, 2541–7 (2005).
1151 76. Alemán, M. *et al.* Mycobacterium tuberculosis-induced activation accelerates apoptosis
1152 in peripheral blood neutrophils from patients with active tuberculosis. *Am. J. Respir.*
1153 *Cell Mol. Biol.* **27**, 583–92 (2002).
1154 77. Perskvist, N., Long, M., Stendahl, O. & Zheng, L. Mycobacterium tuberculosis
1155 promotes apoptosis in human neutrophils by activating caspase-3 and altering
1156 expression of Bax/Bcl-xL via an oxygen-dependent pathway. *J. Immunol.* **168**, 6358–
1157 65 (2002).
1158 78. Chae, H. J. *et al.* Molecular mechanism of staurosporine-induced apoptosis in
1159 osteoblasts. *Pharmacol. Res.* **42**, 373–81 (2000).

1160 79. Zhang, X. D., Gillespie, S. K. & Hersey, P. Staurosporine induces apoptosis of
1161 melanoma by both caspase-dependent and -independent apoptotic pathways. *Mol.*
1162 *Cancer Ther.* **3**, 187–97 (2004).
1163 80. Vermes, I., Haanen, C., Steffens-Nakken, H. & Reutelingsperger, C. A novel assay for
1164 apoptosis. Flow cytometric detection of phosphatidylserine expression on early
1165 apoptotic cells using fluorescein labelled Annexin V. *J. Immunol. Methods* **184**, 39–51
1166 (1995).
1167 81. Pullar, J. M., Vissers, M. C. & Winterbourn, C. C. Living with a killer: the effects of
1168 hypochlorous acid on mammalian cells. *IUBMB Life* **50**, 259–266 (2000).
1169 82. Annibal, A. *et al.* Identification of dityrosine cross-linked sites in oxidized human
1170 serum albumin. *J. Chromatogr. B. Analyt. Technol. Biomed. Life Sci.* **1019**, 147–155
1171 (2016).
1172 83. Cao, W., Hou, F. F. & Nie, J. AOPPs and the progression of kidney disease. *Kidney*
1173 *Int. Suppl.* **4**, 102–106 (2014).
1174 84. Pattison, D. I., Hawkins, C. L. & Davies, M. J. What are the plasma targets of the
1175 oxidant hypochlorous acid? A kinetic modeling approach. *Chem. Res. Toxicol.* **22**,
1176 807–817 (2009).
1177 85. French, K., Yerbury, J. J. & Wilson, M. R. Protease activation of alpha2-macroglobulin
1178 modulates a chaperone-like action with broad specificity. *Biochemistry* **47**, 1176–85
1179 (2008).
1180 86. Rhee, S. G., Kang, S. W., Netto, L. E., Seo, M. S. & Stadtman, E. R. A family of novel
1181 peroxidases, peroxiredoxins. *Biofactors* **10**, 207–209 (1999).
1182 87. Kopprasch, S., Leonhardt, W., Pietzsch, J. & Kühne, H. Hypochlorite-modified low-
1183 density lipoprotein stimulates human polymorphonuclear leukocytes for enhanced
1184 production of reactive oxygen metabolites, enzyme secretion, and adhesion to
1185 endothelial cells. *Atherosclerosis* **136**, 315–24 (1998).

1186 88. Kennedy, A. D. & DeLeo, F. R. PI3K and NADPH oxidase: a class act. *Blood* **112**,
1187 4788–9 (2008).
1188 89. Hawkins, P. T., Davidson, K. & Stephens, L. R. The role of PI3Ks in the regulation of
1189 the neutrophil NADPH oxidase. *Biochem. Soc. Symp.* 59–67 (2007).
1190 doi:10.1042/BSS0740059
1191 90. Binder, V. *et al.* The myeloperoxidase product hypochlorous acid generates irreversible
1192 high-density lipoprotein receptor inhibitors. *Arterioscler. Thromb. Vasc. Biol.* **33**,
1193 1020–1027 (2013).
1194 91. Zhuang, Z. *et al.* The anti-apoptotic effect of PI3K-Akt signaling pathway after
1195 subarachnoid hemorrhage in rats. *Ann. Clin. Lab. Sci.* **41**, 364–72 (2011).
1196 92. Chang, F. *et al.* Involvement of PI3K/Akt pathway in cell cycle progression, apoptosis,
1197 and neoplastic transformation: a target for cancer chemotherapy. *Leukemia* **17**, 590–
1198 603 (2003).
1199 93. Lee, A., Whyte, M. K. & Haslett, C. Inhibition of apoptosis and prolongation of
1200 neutrophil functional longevity by inflammatory mediators. *J. Leukoc. Biol.* **54**, 283–8
1201 (1993).
1202 94. Colotta, F., Re, F., Polentarutti, N., Sozzani, S. & Mantovani, A. Modulation of
1203 granulocyte survival and programmed cell death by cytokines and bacterial products.
1204 *Blood* **80**, 2012–20 (1992).
1205 95. Vossmann, M., Kirst, M., Ludolfs, D. & Schreiber, M. West Nile virus is neutralized
1206 by HOCl-modified human serum albumin that binds to domain III of the viral envelope
1207 protein E. *Virology* **373**, 322–328 (2008).
1208 96. Speth, C. *et al.* Neutrophils turn plasma proteins into weapons against HIV-1. *PLoS*
1209 *One* **8**, e66073 (2013).
1210 97. Weiss, S. J. Tissue destruction by neutrophils. *N. Engl. J. Med.* **320**, 365–376 (1989).
1211 98. Margaroli, C. *et al.* Elastase Exocytosis by Airway Neutrophils Associates with Early

1212 Lung Damage in Cystic Fibrosis Children. *Am. J. Respir. Crit. Care Med.* (2018).
1213 doi:10.1164/rccm.201803-0442OC
1214 99. Erwig, L.-P. & Henson, P. M. Immunological consequences of apoptotic cell
1215 phagocytosis. *Am. J. Pathol.* **171**, 2–8 (2007).
1216 100. Bonham, M. J. *et al.* Early ascorbic acid depletion is related to the severity of acute
1217 pancreatitis. *Br. J. Surg.* **86**, 1296–301 (1999).
1218 101. Ruan, E. A. *et al.* Glutathione levels in chronic inflammatory disorders of the human
1219 colon. *Nutr. Res.* **17**, 463–473 (1997).
1220 102. Huijskens, M. J. A. J., Wodzig, W. K. W. H., Walczak, M., Germeraad, W. T. V &
1221 Bos, G. M. J. Ascorbic acid serum levels are reduced in patients with hematological
1222 malignancies. *Results Immunol.* **6**, 8–10 (2016).
1223 103. Rose, S. *et al.* Evidence of oxidative damage and inflammation associated with low
1224 glutathione redox status in the autism brain. *Transl. Psychiatry* **2**, e134 (2012).
1225 104. Mikirova, N., Casciari, J., Rogers, A. & Taylor, P. Effect of high-dose intravenous
1226 vitamin C on inflammation in cancer patients. *J. Transl. Med.* **10**, 189 (2012).
1227 105. Carr, A. C. & Cook, J. Intravenous Vitamin C for Cancer Therapy - Identifying the
1228 Current Gaps in Our Knowledge. *Front. Physiol.* **9**, 1182 (2018).
1229 106. Block, G. *et al.* Vitamin C treatment reduces elevated C-reactive protein. *Free Radic.*
1230 *Biol. Med.* **46**, 70–7 (2009).
1231

1232 **SUPPLEMENTAL INFORMATION**

1233 **Supplementary Data:** Supplementary Figure 1 and Supplementary Materials and Methods

1234 **Figure 1 – Source Data 1:** Numerical light scattering data obtained during protein
1235 aggregation assays represented in figure 1 a and b

1236 **Figure 2 – Source Data 1:** Numerical light scattering data obtained during protein
1237 aggregation assays represented in figure 2 a and b

1238 **Figure 2 – Source Data 2:** Numerical light scattering data obtained during protein
1239 aggregation assays represented in figure 2 c and d

1240 **Figure 2 – Source Data 3:** Numerical light scattering data obtained during protein
1241 aggregation assays represented in figure 2 e and f

1242 **Figure 3 – Source Data 1:** Numerical fluorescence spectroscopy data obtained during
1243 determination of free amino groups represented in figure 3 a and b

1244 **Figure 3 – Source Data 2:** Numerical fluorescence spectroscopy data obtained during
1245 determination of protein hydrophobicity represented in figure 3 c

1246 **Figure 3 – Source Data 3:** Numerical fluorescence spectroscopy intensity data obtained
1247 during determination of protein hydrophobicity represented in figure 3 d

1248 **Figure 4 – Source Data 1:** Numerical chemiluminescence plate reader data represented in
1249 figure 4 a, b, and c

1250 **Figure 5 – Source Data 1:** Numerical light scattering data obtained during protein
1251 aggregation assays represented in figure 5 a and b

1252 **Figure 5 – Source Data 2:** Numerical light scattering data obtained during protein
1253 aggregation assays represented in figure 5 c and d

1254 **Figure 5 – Source Data 3:** Numerical light scattering data obtained during protein
1255 aggregation assays represented in figure 5 e and f

1256 **Figure 6 – Source Data 1:** Numerical chemiluminescence plate reader data represented in
1257 figure 6 a and b

1258 **Figure 6 – Source Data 2:** Numerical chemiluminescence plate reader data represented in
1259 figure 6 c and d
1260 **Figure 6 – Source Data 3:** Numerical chemiluminescence plate reader data represented in
1261 figure 6 e and f
1262 **Figure 7 – Source Data 1:** Numerical chemiluminescence plate reader data represented in
1263 figure 7 a and d
1264 **Figure 7 – Source Data 2:** Numerical chemiluminescence plate reader data represented in
1265 figure 7 b and d
1266 **Figure 7 – Source Data 3:** Numerical chemiluminescence plate reader data represented in
1267 figure 7 c and d
1268 **Figure 8 – Source Data 1:** Numerical flow cytometry data represented in figure 8 a and b
1269 **Figure 9 – Source Data 1:** Numerical light scattering data obtained during protein
1270 aggregation assays represented in figure 9 a and b
1271 **Figure 9 – Source Data 2:** Numerical flow cytometry data obtained during protein
1272 aggregation assays represented in figure 9 c and d